Fungal resistance mediated by maize wall-associated kinase Zm WAK-RLK1 correlates with reduced benzoxazinoid content

Yang, Ping ; Praz, Coraline ; Li, Beibei ; Singla, Jyoti ; Robert, Christelle A M ; Kessel, Bettina ; Scheuermann, Daniela ; Lüthi, Linda ; Ouzunova, Milena ; Erb, Matthias ; Krattinger, Simon G ; Keller, Beat

Abstract: Wall-associated kinases (WAKs) have recently been identified as major components of fungal and bacterial disease resistance in several cereal crop species. However, the molecular mechanisms of WAK-mediated resistance remain largely unknown. Here, we investigated the function of the maize gene ZmWAK-RLK1 (Htn1) that confers quantitative resistance to northern corn leaf blight (NCLB) caused by the hemibiotrophic fungal pathogen Exserohilum turcicum. ZmWAK-RLK1 was found to localize to the plasma membrane and its presence resulted in a modification of the infection process by reducing pathogen penetration into host tissues. A large-scale transcriptome analysis of near-isogenic lines (NILs) differing for ZmWAK-RLK1 revealed that several differentially expressed genes are involved in the biosynthesis of the secondary metabolites benzoxazinoids (BXs). The contents of several BXs including DIM2BOA-Glc were significantly lower when ZmWAK-RLK1 is present. DIM2BOA-Glc concentration was significantly elevated in ZmWAK-RLK1 mutants with compromised NCLB resistance. Maize mutants that were affected in overall BXs biosynthesis or content of DIM2BOA-Glc showed increased NCLB resistance. We conclude that Htn1-mediated NCLB resistance is associated with a reduction of BX secondary metabolites. These findings suggest a link between WAK-mediated quantitative disease resistance and changes in biochemical fluxes starting with indole-3-glycerol phosphate.

DOI: https://doi.org/10.1111/nph.15419

Fungal resistance mediated by maize wall-associated kinase ZmWAK-RLK1 correlates with reduced benzoxazinoid content

Ping Yang[1,4], Coraline Praz[1], Beibei Li[2], Jyoti Singla[1], Christelle Robert[2], Bettina Kessel[3], Daniela Scheuermann[3], Linda Lüthi[1], Milena Ouzunova[3], Matthias Erb[2*], Simon G. Krattinger[1,5*], Beat Keller[1*]

[1]Department of Plant and Microbial Biology, University of Zurich, Zollikerstrasse 107, CH-8008 Zurich, Switzerland

[2]Institute of Plant Sciences, University of Bern, CH-3013 Bern, Switzerland

[3]KWS SAAT SE, DE-37574 Einbeck, Germany

[4]Institute of Crop Sciences, Chinese Academy of Agricultural Sciences, 100081 Beijing, China

[5]King Abdullah University of Science and Technology, Thuwal, Kingdom of Saudi Arabia

[*]Authors for correspondence:

Beat Keller; Tel: +41 446348230; E-mail: bkeller@botinst.uzh.ch

Simon G. Krattinger; Tel: +41 446348233; E-mail: skratt@botinst.uzh.ch

Matthias Erb, Tel: +41 316318668; E-mail: matthias.erb@ips.unibe.ch

ORCID IDs:

Ping Yang: https://orcid.org/0000-0002-6977-8449

Simon G. Krattinger: https://orcid.org/0000-0001-6912-7411

Beat Keller: https://orcid.org/0000-0003-2379-9225

Words for the main body of the text: 5056

Words for Introduction: 812

Words for Materials and Methods: 1668

Words for Results: 1406

Words for Discussions: 1087

Words for Acknowledgement: 83

Number of figures: 6

Supporting information: 4 tables and 11 figures

Data deposition: The sequences reported in this paper have been deposited in the NCBI database (Accession No.: GSE100667).

Conflict of interest statement: A patent application has been filed relating to this work.

Brief heading: NCLB resistance mediated by ZmWAK-RLK1 correlates with benzoxazinoid reduction.

Summary

- Wall associated kinases (WAKs) have recently been identified as major components of fungal and bacterial disease resistance in several cereal crop species. However, the molecular mechanisms of WAK-mediated resistance remain largely unknown.
- Here, we investigated the function of the maize gene *ZmWAK-RLK1* (*Htn1*) that confers quantitative resistance to northern corn leaf blight (NCLB) caused by the hemibiotrophic fungal pathogen *Exserohilum turcicum*.
- ZmWAK-RLK1 was found to localize to the plasma membrane and its presence resulted in a modification of the infection process by reducing pathogen penetration into host tissues. A large-scale transcriptome analysis of near-isogenic lines (NILs) differing for *ZmWAK-RLK1* revealed that several differentially expressed genes that are involved in the biosynthesis of the secondary metabolites benzoxazinoids (BXDs). The contents of several BXDs including DIM_2BOA-Glc were significantly lower when *ZmWAK-RLK1* is present. DIM_2BOA-Glc concentration was significantly elevated in *ZmWAK-RLK1* mutants with compromised NCLB resistance. Maize mutants that were affected in overall BXDs biosynthesis or content of DIM_2BOA-Glc showed increased NCLB resistance.
- We conclude that *Htn1*-mediated NCLB resistance is associated with a reduction of BXD secondary metabolites. These findings suggest a link between WAK-mediated quantitative disease resistance and changes in biochemical fluxes starting with indole-3-glycerol phosphate.

Key words: Wall-associated kinase, receptor-like kinase, benzoxazinoids (BXDs), maize disease resistance, *Htn1*

Introduction

Plants have evolved multiple layers of defense against infection by pathogenic microbes (Jones & Dangl, 2006; Krattinger & Keller, 2016). The primary defense is based on the extracellular perception of pathogen-derived or host damage-derived signatures (PAMPs/DAMPs) by plasma membrane-localized receptors. These signatures can be highly conserved and characteristic for entire pathogen classes as in the case of the bacterial flagellin that is perceived by the leucine-rich repeat receptor kinase (LRR-RK) FLS2, which results in basal and broad-spectrum resistance against most bacteria (Dardick *et al.*, 2012; Macho & Zipfel, 2014). Other receptor kinases only confer resistance to certain races of a particular pathogen (Hu *et al.*, 2017). Receptor kinases have different types of extracellular domains, including leucine-rich repeats, lysine motifs, lectin motifs or epidermal growth factor like extracellular domains (Gomez-Gomez & Boller, 2000; Dardick *et al.*, 2012; Macho & Zipfel, 2014). The wall-associated kinases (WAKs) contain a cell wall-associated galacturonan-binding domain (Kanneganti & Gupta, 2008). In grasses, there is emerging evidence that WAKs are important players in fungal and bacterial disease resistance. The WAK genes *ZmWAK* (*qHSR1*), *ZmWAK-RLK1* (*Htn1*) and *OsWAK* (*Xa4*) confer disease resistance against maize head smut, maize northern corn leaf blight (NCLB) and rice bacterial blight, respectively (Hurni *et al.*, 2015; Zuo *et al.*, 2015; Hu *et al.*, 2017). *WAK*-mediated resistance involves strengthening of the cell wall intensity by enhancing cellulose biosynthesis and the biosynthesis of phytoalexin (Hu *et al.*, 2017), oxidative burst (Delteil *et al.*, 2016), and defense gene expression (Zuo *et al.*, 2015). Interestingly, there is also one case described where the wheat WAK encoded by the *Snn1* gene acts as a susceptibility factor. It has been shown that Snn1 perceives the SnTox1 toxin encoded by the fungal pathogen *Parastagonospora nodorum*, which triggers cell death and allows the necrotrophic *P. nodorum pathogen* to proliferate on wheat (Shi *et al.*, 2016). In dicots, the Arabidopsis AtWAK1 was found to physically associate with and to recognize cell wall-derived oligogalactouronides, which result from polysaccharide degradation (Decreux *et al.*, 2006; Brutus *et al.*, 2010).

Indole-3-glycerol phosphate (IGP) is an important metabolite and serves as a branch point compound in the Trp-independent biosynthesis of the plant auxin indole-3-acetic acid (IAA) and the biosynthesis of defense-related benzoxazinoids (BXDs) (Frey *et al.*, 2000; Di *et al.*, 2016). Benzoxazinoids (BXDs) are a class of secondary metabolites found in maize and other cereal species that contain the 2-hydroxy-2H-1,4-benzoxazin-3(4H)-one skeleton (Niemeyer, 2009; Wouters *et al.*, 2016). The biosynthesis of BXDs is mostly under developmental control (Kohler *et al.*, 2015). The first step of BXDs synthesis is based on the formation of indole derived from indole-3-glycerol phosphate (IGP), converted by indole-glycerolphosphate lyase BX1 (Frey *et al.*, 2000). In addition to BX1, its homolog IGL can convert IGP into free indole (Frey *et al.*, 2000; Niemeyer, 2009). BXD metabolism largely depends on the content of indole and *Igl* can contribute up to 10% of total BXDs levels (Frey *et al.*,

2000). After several successive steps of oxidation and methylation, predominantly inactive glucosides are produced and stored as vacuolar BXDs (*e.g*. DIMBOA-Glc). Upon biotic stress they are hydrolyzed to the respective toxic active hydroxamic acids (e.g. DIMBOA) (Niemeyer, 2009; Wouters *et al.*, 2016). These compounds are known to be involved in defense against aphids, phloem-feeding herbivores and other pests (Niemeyer, 2009), for instance the European corn borer *Ostrinia nubilalis* and the cereal aphid *Rhopalosiphum padi* (Houseman *et al.*, 1992; Ahmad *et al.*, 2011). However, certain herbivores can circumvent benzoxazinoid toxicity and use BXDs as foraging cues (Robert *et al.*, 2012; Kohler *et al.*, 2015; Wouters *et al.*, 2016).

While the role of BXDs in insect resistance is quite well studied, the role of these compounds in fungal disease resistance remains unclear. Several field studies proposed a relationship between active benzoxazinoid hydroxamic acid DIMBOA and the disease resistance to maize stalk rot, maize NCLB and wheat stem rust (Elnaghy & Pekka, 1962; Long *et al.*, 1978; Kostandi *et al.*, 1981). Induction of DIMBOA accumulation possibly associated to the increased sheath blight disease caused by *Rhizoctonia solani* (Song *et al.*, 2011). However, other studies found no effect of BXDs on fungal disease resistance, including maize stalk rot, southern corn leaf blight, maize anthracnose, corn smut and head blight (Niemeyer, 2009). Recently, *E. turcicum,* the causal agent of NCLB, has been shown to elicit apoplastic BXDs accumulation at the early infection stages (Ahmad *et al.*, 2011), which suggested a link between BXDs and *E. turcicum* infection. This study suggested an inhibition of penetration success however did not show whether BXDs contribute to increased disease resistance or susceptibility.

We recently isolated by map-based cloning the maize *Htn1* gene that encodes a putative wall-associated receptor-like kinase (Hurni *et al.*, 2015). Unlike the dominant gene *Ht1* that causes hypersensitive response-like chlorotic lesions (Welz & Geiger, 2000), *Htn1* confers quantitative and partial resistance against NCLB by delaying lesion formation and sporulation (Hurni *et al.*, 2015). In this study, we investigated the molecular basis of quantitative NCLB resistance conferred by *ZmWAK-RLK1* (*Htn1*). We provide evidence that NCLB resistance caused by *ZmWAK-RLK1* is associated with a reduction of secondary metabolite benzoxazinoids, a biochemical pathway of IGP metabolism.

Materials and Methods

Plant material and growth conditions

Nineteen maize inbred lines were used in the study, including: (1) historical cultivars B37 and w22, and the NILs B37Htn1 and w22Htn1 that contain the NCLB resistance gene *Htn1* (Table S1), which were originally developed via crossing the donor line “Pepitilla” (a Mexican landrace) and the recurrent parental lines by Mr. Raymundo and colleagues from University of Illinois (Raymundo *et al.*,

1981); (2) Breeding line RP3 and its NIL RP3Htn1 carrying *Htn1* (KWS, Einbeck, Germany); (3) three pairs of mutants RLK1b (1365', G to A, Met to Ile), RLK1d (1490', C to T, Leu to Phe) and RLK1f (1642', G to A, Gly to Arg, susceptible/compromised resistance), and their corresponding sister lines RLK1b-wt, RLK1d-wt, and RLK1f-wt (resistant, carrying functional *Htn1*), which were produced by EMS-mutagenesis in RP3Htn1 (Hurni *et al.*, 2015); (4) three maize mutants (bx1, bx2 and bx6) and parental line w22 (referred w22-wt, in order to make difference with the line w22, provided by KWS), which were kindly provided by Prof. Georg Jander (Cornell University, Ithaca, US); (5) the NILs Bx13NIL-B73 that contains a functional *Bx13* allele and Bx13NIL-Oh43 that contains non-functional *bx13* allele compromising the synthesis of DIM_2BOA-Glc (Handrick *et al.*, 2016).

NCLB infection tests in the greenhouse

Testing for NCLB resistance using *E. turcicum* isolate Passau-1 was performed as previously described with minor modification (Yang *et al.*, 2017). Two or three maize seeds were sown in a Jiffy pot (ø 8cm), and fifteen pots were placed in one tray. Seedling plants were grown in a greenhouse (16 h at 20°C in the day, 8 h at 18°C in the night and approximately 60% relative humidity). After the second leaves had fully emerged, the later emerging leaves were cut and removed until the end of each experiment. Single spore inoculation and culture on PDA medium plate, harvest and quantification of progeny spores were performed as described (Yang *et al.*, 2017). Instead of infection by dropping 80 µl spore suspension into the leaf sheath of the second leaf twice, here maize seedlings were infected once by spray (sprayer: ø 28mm, Semadeni, Ostermundigen, Switzerland). Each 4 trays (ca. 60-80 seedlings) were sprayed with 4 ml of spore suspension (4.5×10^4 spores/ml). A very high humidity micro-condition was produced by placing plastic hoods on top of each tray after infection. Each plant was scored for disease symptoms between 11 and 25 days and the severity was evaluated by calculating the area under the disease progress curve (AUDPC) or by quantifying the diseased leaf area of the inoculated second leaves (PrimDLA) (Yang *et al.*, 2017). About 15 seedling plants were scored for each genotype in each experiment.

Test for insect performance in the greenhouse

Spodoptera littoralis and *Diabrotica balteata* eggs were kindly provided by Ted Turlings (University of Neuchâtel, CHE) and Oliver Kindler (Syngenta Crop Protection, Stein), respectively. For insect feeding assay, maize plants were sown in 1 L pots and grown under greenhouse condition (350 umol.m-2.s-1 light, 14 h day, 55% relative humidity, 26±2°C). Plants with four fully developed leaves were used for the experiments. Three pre-weighed second-instar larvae of *S. littoralis* or *D. balteata* were added to w22 and w22Htn1 plants. Control plants remained uninfested. Modified PET bottles were added on all individual plants as previously described (Erb *et al.*, 2011). After 8 days, all larvae were collected

158 and weighed again to calculate their relative weight gain. Larval survival rate was calculated based on
159 the proportion of larvae recovered per pot.

160 **Vector construction, subcellular localization and western blotting**

161 The coding sequence of *ZmWAK-RLK1* was amplified using a cDNA clone as template, which was
162 initially amplified in NCLB resistance line RP1Htn1 (Hurni *et al.*, 2015). The primers used for this
163 construct are given (Table S2). The PCR fragment was introduced into the Gateway donor vector
164 pDONR207 using the Gateway® BP Clonase® II Enzyme mix (Thermo Fisher Scientific, Wilmington,
165 USA). The generated entry vector carrying the target *ZmWAK-RLK1* sequence was inserted by
166 recombination in the destination vector pUBC-GFP-DEST, to produce an in-frame *ZmWAK-RLK1* + c'-
167 eGFP fusion protein construct driven by the Arabidopsis ubiquitin-10 (UBQ10) gene promoter
168 (Grefen *et al.*, 2010). The *UBQ10:: ZmWAK-RLK1-c'-eGFP* construct together with a reference plasmid
169 PIP2A-mCherry (contains *35S::PIP2A_c'_RFP* construct, which is localized to the plasma membrane)
170 (Nelson *et al.*, 2007) were mixed with nanograde gold particles and co-bombarded into onion
171 epidermal cells, which were subsequently incubated at 20°C in the dark for 2-3 days until being ready
172 for observation using a Zeiss LSM 880 confocal microscope (CARL ZEISS, Jena, Germany) by following
173 the standard instructions. Plasmolysis was induced by adding a 0.8 M mannitol solution.

174 The same plasmids were transformed into Agrobacterium GV3101 and co-infiltrated into 4-week-old
175 *N. benthamiana* leaves, which were ready for observation 2 days post infiltration. The
176 *Agrobacterium*-infiltrated tobacco leaves were harvested for the extraction of total proteins using
177 the lysis buffer (150 mM NaCl, 50 mM Tris-HCl at pH 7.5, 5 mM EDTA at pH 8.0, 0.1% Triton X-100,
178 0.2% NP-40) plus freshly added PMSF (phenylmethylsulphonyl fluoride, 10 mM). The GFP-tagged
179 protein was checked by western blotting using anti-GFP antibody (1:2000, Roche, 11814460001).

180 Maize protoplasts were isolated from the second leaves of maize seedling plants. After seed sowing,
181 these maize plants were planted 10-14 days under dark condition. Transformation of plasmid
182 constructs was following standard methods (Yoo *et al.*, 2007), and the protoplasts were incubated for
183 24-48 hours under dark condition until being ready for observation using the confocal microscope.

184 **Analysis of *E. turcicum* infection**

185 The second leaves of 21-day seedling plants were harvested and cut into 2 × 2 cm^2 leaf segments,
186 which were placed and incubated on phytoagar plates. A spore suspension (4.5×10^4 spores/ml) was
187 painted on the leaf surface using swabs. The petri dishes carrying samples were sealed using
188 PARAFILM and incubated for 24 hours at room temperature until harvest.

189 Trypan blue staining was conducted as previously described (Chung *et al.*, 2010). The infected
190 segments at 1 dpi were incubated overnight in an acetic acid: ethanol (1:3, v/v) solution, and then in

a mixed solution of acetic acid : ethanol : glycerol (1:5:1, v/v/v) for 4 hours. The samples were stained overnight in 0.01% (w/v) trypan blue lactophenol solution, and then washed once using ddH_2O and stored in 60% glycerol ready for use. Specimens were placed on slides and examined under the ZEISS Axio Imager 2 microscope system (CARL ZEISS, Jena, Germany) with normal light, by magnifying 10 or 20 times. In general, more than 50 spores were counted in each replicate of each sample, and at least three specimens were checked. The numbers of germinated spores, germ tubes, appressoria and successful penetrations (hyphae inside of cell or between cell walls) were counted. Three independent experiments were performed.

RNA extraction, RNA sequencing and data analysis

The second leaves of seedling plants were harvested with four biological replicates at 0, 9-hpi, 3-dpi and 10-dpi, which corresponded to before inoculation, the germination/penetration, biotrophic growth and necrotrophic growth, respectively (Jennings & Ullstrup, 1957; Hilu & Hooker, 1964). Forty-eight samples (4 genotypes, 4 time points, 3 biological replicates) were subjected for total RNA extraction using SV Total RNA Isolation Kits (Promega, Dübendorf, Switzerland). 1 µl of total RNA was checked by Nanodrop 1000 Spectrophotometer (Thermo Fisher Scientific, Wilmington, USA) to estimate the RNA concentration. Meanwhile, 15 plants in each genotype were evaluated for the AUDPC value to control if the infection worked.

The quantity and quality in RNA for RNA sequencing were determined using Qubit® 1.0 Fluorometer (Thermo Fisher Scientific, Wilmington, USA) and Bioanalyzer 2100 (Agilent, Waldbronn, Germany). The TruSeq Stranded mRNA Sample Prep Kit (Illumina, Inc., Hayward, USA) was used for library preparation. 1 µg of total RNA per sample was ribosome depleted and then subjected for synthesizing double-strand cDNA. Each cDNA sample was fragmented, end-repaired, polyadenylated and then ligated with TruSeq adaptor that contains the index for multiplexing. The cDNA fragments containing TruSeq adapters at the both ends were enriched with PCR reaction. The enriched libraries were quantified and qualified, and then normalized to 10 nM. The TruSeq SR Cluster Kit v4 cBot (Illumina, Inc., Hayward, USA) was used for cluster generation using 8 pM of pooled normalized libraries. Sequencing was performed on the Illumina HiSeq2500 at single end 125 bp using the TruSeq SBS Kit v4 (Illumina, Inc., Hayward, USA).

The maize reference genome Zea_mays.AGPv3.27 and the corresponding annotation were downloaded (http://www.maizegdb.org/). The RNA sequencing reads were mapped on the reference genome with STAR (Dobin *et al.*, 2013) allowing one mismatch per 100 bp and no multimappers with the following command: STAR -outFilterMultiMapNmax 1 - outFilterMismatchNoverLmax 0.01 - alignIntronMax 10000. Read counts were determined from the mapping files with featureCounts 1.4.6 (Liao *et al.*, 2014) using standard parameters with the command “featureCounts bam -a gtf”.

Statistical analyses were done with the R package edgeR and genes were tested for differential expression with pairwise comparisons and tagwise estimation of dispersion (Robinson *et al.*, 2010). A gene was considered to be expressed when at least 10 reads were mapped on it and a gene was considered to be differentially expressed with $\log_2FC \geq |2|$ and FDR < 0.01. First, pairwise comparisons were performed between NILs with/without *Htn1* for each genotype and each time point separately. The results were then compared between time points and then between the two genotypes. The Gene Ontology analysis for DEGs was conducted by using online software agriGO (Du *et al.*, 2010). The significant terms were colored if adjusted $p \leq 0.05$.

RT-qPCR assay

1µg total RNA was subjected for first strand cDNA synthesis using the iScript Advanced cDNA kit (172-5038, Rio-Rad). 1:20 diluted cDNA was applied for quantifying expression using a Real-Time System C1000TM Thermal cycler (96 or 384 wells, Bio-Rad). The expression of targets was normalized by the reference genes *FPGS* and *Actin* as described (Balmer *et al.*, 2013; Hurni *et al.*, 2015). The primers for expression analysis are shown (Table S2).

Benzoxazinoids extraction and measurement

60 - 100 mg leaves (without veins) of the seedling plants were harvested and frozen immediately in liquid nitrogen, grinded and extraction buffer was added (1 mg sample + 10 µl extraction buffer). The samples were mixed thoroughly and centrifuged at 15,871 g at 4˚C. The supernatant was transferred into a new tube and centrifuged once more under the same condition to remove leaf particles. The supernatant was collected for BXD measurements.

Benzoxazinoid contents were analyzed by an Acquity UPLC equipment (Waters) coupled to a UV detector and a mass spectrometer (Waters) (Meihls *et al.*, 2013). An Acquity BEH C18 column (Waters) was used. The temperatures of the autosampler and column were 15 °C and 40 °C, respectively. The mobile phase consisted of 99% water, 1% acetonitrile, and 0.1% formic acid (A) and acetonitrile and 0.1% Formic acid (B). Flow rate was set to 0.4 ml min^{-1} with 3% A and 97% B followed by column reconditioning. The injection volume was 5 µl. The extracted trace at 275 nm was used for benzoxazinoids quantification. The following extracted ion chromatograms were used for quantification with a mass window of ±0.01 D: mass-to-charge ratio (m/z) for DIMBOA (retention time [RT] 5.62 min) and DIMBOA-Glc (RT 5.64 min), m/z for HDMBOA-Glc (RT 8.19 min), m/z for HMBOA-Glc (RT 5.34 min), m/z for DIM_2BOA-Glc (RT 5.825 min) and HDM_2BOA-Glc (RT 8.32 min). Benzoxazinoids absolute concentrations were determined by external calibration curves obtained from purified DIMBOA-Glc, DIMBOA and HDMBOA-Glc standards. TRIMBOA-Glc and HDM_2BOA-Glc are below than the detection limit and not shown.

Results

ZmWAK-RLK1 encodes a plasma membrane localized protein

To determine the subcellular localization of the ZmWAK-RLK1 protein, we generated a fusion construct consisting of a full-length coding sequence fused to the sequence of an enhanced green fluorescence protein at the C terminus (Grefen *et al.*, 2010). The ZmWAK-RLK1 fusion protein localized to the plasma membrane before and after plasmolysis when transiently expressed in onion epidermal cells (Fig. 1A-B). Secondly, infiltration into leaves of *Nicotiana benthamiana* indicated the localization of ZmWAK-RLK1 to the plasma membrane two days after infiltration (Fig. 1C). A fusion protein of ZmWAK-RLK1 and GFP was detected by western blot analysis (Fig. S1). Thirdly, we transiently expressed the same gene fusion in maize protoplasts. The encoded protein was found to be localized to the plasma membrane 36 hours after transformation (Fig. 1D). Thus, these data indicate that ZmWAK-RLK1 is a plasma membrane-localized protein.

ZmWAK-RLK1 reduces fungal penetration rate

Spores of the hemibiotrophic fungus *E. turcicum* penetrate the maize epidermis mostly between 6-18 hours after inoculation (hpi) (Jennings & Ullstrup, 1957; Hilu & Hooker, 1964). To investigate if *ZmWAK-RLK1* changes the outcome of fungal penetration attempts, we investigated the infection process at one day post inoculation (dpi) using trypan blue staining (Fig. 2A and Fig. S2A-C). The numbers of successful penetration events were evaluated in three EMS-induced *ZmWAK-RLK1* loss-of-function mutant lines (RLK1b, RLK1d and RLK1f) and their corresponding sister lines that were generated in the near isogenic line (NIL) RP3Htn1 (Table S1) (Hurni *et al.*, 2015). No significant differences in the establishment of germ tubes and appressoria were observed in mutants and sister lines (Fig. S2D-E). In contrast, the number of successful penetration events was significantly lower if *ZmWAK-RLK1* was functional compared to loss-of-function mutants at 1 dpi (Fig. 2B). In order to compare the penetration ratio at different days post inoculation, we counted the penetration events at 1 dpi and 3 dpi in genotype B37 and NIL B37Htn1. The rate of successful penetration significantly decreased at 3 dpi vs 1 dpi (Fig. 2C). This indicates that *ZmWAK-RLK1* plays role in reduction of pathogen penetration into host tissues, in agreement with the partial resistance/delayed susceptibility.

Transcriptome and metabolism analysis identifies alterations of the benzoxazinoids (BXDs) biosynthesis pathway in the presence of *ZmWAK-RLK1*

The surface-localized RLKs act as crucial components in plant immune signaling (Zipfel *et al.*, 2017). In order to decipher the transcriptional regulation network specifically influenced by *ZmWAK-RLK1*, we performed a transcriptome analysis by RNA sequencing in two pairs of near isogenic lines, w22 and

w22Htn1 as well as B37 and B37Htn1. NCLB development was significantly reduced in the presence of *ZmWAK-RLK1* in both NILs (Fig. S3A-C). Leaf samples were collected at 0 and 9 hpi (penetration stage) as well as 3 dpi (biotrophic growth) and 10 dpi (necrotrophic growth) (Jennings & Ullstrup, 1957; Hilu & Hooker, 1964). Forty-eight samples were sequenced and 1.159 billion reads were obtained (Table S3). More than 820 million reads were uniquely mapped with an average of 17.08 million reads per sample (70.7% of total reads) (Table S3). A total of 15,345 genes were expressed and they were used for further analysis. By conducting a multidimensional scaling analysis using expression normalized by reads per kilobase per million mapped reads (RPKM) using edgeR, the biological replicates for the same genotype-time point combinations mostly grouped together, demonstrating high similarity of replicates (Fig. S4A-C). A high number of differentially expressed genes (DEGs) was detected in B37Htn1/B37 compared to w22Htn1/w22 (Fig. S5A). To identify DEGs associated with *ZmWAK-RLK1* and to rule out genetic background effects, only genes that were differentially expressed in both NIL pairs were further considered.

Two-hundred and fifteen common DEGs were identified across all time points (Table S4). 132 and 83 genes were induced and repressed, respectively, in NILs with *ZmWAK-RLK1* compared to the parental lines without *ZmWAK-RLK1* (Fig. S5B-C). An overrepresentation analysis using agriGO revealed an enrichment of Gene Ontology (GO) terms associated with defense response (e.g. GO:0009814) and metabolic/biosynthetic process (e.g. GO:0006725) (Fig. S6). Twenty-nine DEGs were differently expressed at all time points including time point 0 (Fig. S5C). Using the annotation information of the best hit rice homologs, four genes were annotated as hypersensitive induced response protein (GRMZM2G157869) and receptor-like kinase proteins (GRMZM2G433684, GRMZM2G165387, GRMZM2G436455) that might indicate an association with disease resistance. We then considered all the 215 DEGs that have available annotation information in maize. Several DEGs were found and belonged to known pathways that are associated with disease resistance, including biosynthesis of the defense hormones jasmonic acid (JA) and ethylene as well as lignin and cell wall biosynthesis (Table S4). Interestingly, we found five DEGs that are part of the BXDs biosynthesis pathway. This finding was surprising because these secondary metabolites have been mainly described to increase plant resistance against insects (Niemeyer, 2009; Wouters *et al.*, 2016). The five genes *Bx2*, *Igl-like*, *Bx6*, *Bx11* and *Bx14* showed differential expression in at least one time point (Table S4).

To analyze if the presence of *ZmWAK-RLK1* is associated with lower BXD content, BXDs were quantified in the second leaves of w22Htn1 and w22 before and after infection (Fig. 3A-F). The content of the four BXDs DIMBOA-Glc, DIMBOA, HMBOA-Glc and DIM_2BOA-Glc was significantly lower in w22Htn1 compared to w22 at all time points (Fig. 3B-E), which indicated a constitutive reduction of BXD accumulation in the presence of *ZmWAK-RLK1*. Furthermore, we determined by RT-qPCR the transcriptional levels of *ZmWAK-RLK1* and specifically the genes in the BXDs biosynthesis

pathway before and after pathogen inoculation (Fig. S7A-P). Both the expression of *ZmWAK-RLK1* and of the BXD genes *Bx1*, *Bx6* and *Bx13* were lower in w22Htn1 (Fig. S7B, S7H and S7N).

To test if the lower BXD content in w22Htn1 impaired resistance against herbivores, we evaluated maize lines w22 and w22Htn1 upon infections with leaf-feeding *Spodoptera littoralis* and root-feeding *Diabrotica balteata* (Fig. S8A-F). Although the aboveground biomass of w22Htn1 plants was lower than of w22 plants, food was not restricted for *S. littoralis* larvae. No difference in the growth of the two generalist herbivores was noted (Fig. S8A-F).

Taken together, our data indicate a reduced content of BXDs in the presence of *ZmWAK-RLK1*.

Mutations in BXDs biosynthesis genes increase NCLB resistance

To further analyze a possible positive or negative role of BXD biosynthesis genes in NCLB resistance, mutants in the three genes *Bx1*, *Bx2* and *Bx6* in the w22 genetic background (Vollbrecht *et al.*, 2010) were tested for disease development after inoculation with *E. turcicum* (Fig. 4A). These mutants showed strong reduction in several BXDs compounds (Fig. S9). For example, HMBOA-Glc became nearly undetectable in mutants and DIMBOA was reduced by more than 80%. Interestingly, by quantifying disease severity using AUDPC, all three mutants showed an increase in NCLB resistance in five-week old plants if compared to susceptible genotype w22 (Fig. 4A-B). This confirmed a negative association of BXDs content and NCLB disease resistance. Furthermore, we checked the *ZmWAK-RLK1* expression at 10 dpi (Fig. 4C). No significant difference was detected in the *bx* mutants if compared to the wild-type.

Compromising the synthesis of DIM_2BOA-Glc increases NCLB resistance

In addition, we tested for NCLB resistance in Bx13NIL-B73 that contains a wild type functional *Bx13* allele and Bx13NIL-Oh43 that contains a non-functional *bx13* allele. This mutation results in a frame shift mutation in *Bx13* that specifically compromised the synthesis of DIM_2BOA-Glc and its downstream compound HDM_2BOA-Glc (TRIMBOA-Glc was below the detection limit), without modified contents of BXD compounds upstream in the biosynthetic (Handrick *et al.*, 2016). Interestingly, in the *bx13* mutant, we found an increase in NCLB resistance during the early infection phase (Fig. 5).

Mutations in *ZmWAK-RLK1* are associated with the induction of the secondary metabolite DIM_2BOA-Glc

To further analyze the role of different BXD biosynthesis genes as well as the metabolites of this pathway in NCLB resistance, EMS-induced mutants of *ZmWAK-RLK1* and their sister lines in RP3 background were used (Hurni *et al.*, 2015). We quantified the content of major BXD compounds and

the transcript levels of several BXD genes in mutants which lost the resistance caused by *ZmWAK-RLK1*. The content of DIM_2BOA-Glc in mutants relative to sister lines was significantly higher (Fig. 6A), while we didn't observe consistent pattern on contents of other BXD compounds (Fig. S10). The induction of DIM_2BOA-Glc content associated with higher *Igl* transcript level (Fig. 6B), while no obvious difference in the transcriptional levels of *ZmWAK-RLK1* and *Bx1* was detected in mutants and sister lines (Fig. S11A-B). *Bx6*, *Bx7* and *Bx13* are key genes of the BXDs pathway to produce DIM_2BOA-Glc, and these genes were slightly but not significantly upregulated when *ZmWAK-RLK1* is present (Fig. S11C-E). This phenomenon can be explained by a feedback regulation, which has been proposed in BXD metabolism pathways (Ahmad *et al.*, 2011). We conclude that in RP3 genetic background, *ZmWAK-RLK1* is associated with the reduction of secondary metabolite DIM_2BOA-Glc and the reduction of the expression levels of *Igl*.

Taken together, our results indicated that *ZmWAK-RLK1* underlying quantitative NCLB disease resistance is associated to a decrease of the biosynthesis of secondary metabolite BXDs (*e.g.* DIM_2BOA-Glc), which are involved in biochemical pathways starting with indole-3-glycerol phosphate.

Discussion

In this study, we investigated the functional basis of quantitative resistance to northern corn leaf blight of maize mediated by the wall-associated kinase ZmWAK-RLK1 encoded by the *Htn1* gene (Hurni *et al.*, 2015). Our work here provides evidence that *ZmWAK-RLK1* is associated with the reduction of BXDs. BXDs have been found in many cereal species such as maize and wheat, which are important food crops worldwide (Niemeyer, 2009).

Two earlier studies suggested a positive association of BXDs compound DIMBOA and resistance against *E. turcicum* spore germination and penetration (Couture *et al.*, 1971; Ahmad *et al.*, 2011). Infections by either *E. turcicum* or *B. maydis* resulted in the elevation of BXDs (e.g. HDMBOA-Glc) (Ahmad *et al.*, 2011; Oikawa *et al.*, 2004). In contrast, our results revealed no significant difference of the content of HDMBOA-Glc (0 and 3 dpi), but the reduction of several BXD compounds (DIMBOA, DIMBOA-Glc, DIM_2BOA-Glc) in five week old plants of genotypes w22 and w22Htn1. An increase of northern corn leaf blight resistance was observed in BXD-deficient mutants. The former study was conducted on 8 days old seedlings (Ahmad *et al.*, 2011), and the discrepancy might be due to the difference in BXD content between the two developmental stages (Kohler *et al.*, 2015). Although BXDs were significantly lower in w22 relative to w22Htn1, we did not detect any difference on the performance and biomass removal for the insect pests *S. littoralis* and *D. balteata*. This is surprising given the described role of BXDs in resistance to these two herbivores (Niemeyer, 2009; Wouters *et al.*, 2016). This might be explained by the presence of an *Htn1*-independent resistance factor which

compensates for the lower BXD content. Alternatively, the herbivores might induce BXDs synthesis to similar levels.

Furthermore, a *Bx13* knock-out mutant that blocks the synthesis of DIM_2BOA-Glc and/or HDM_2BOA-Glc has been shown to result in 50% more progeny of corn leaf aphids *Rhopalosiphum maidis*, but showed no difference on the weight of chew feeding insects *S. littoralis*, *S. exigua* and *D. balteata* in feeding experiments (Handrick *et al.*, 2016). That suggests a functional specificity of DIM_2BOA-Glc that interplays with negative effects on aphid growth only. Our resulted confirmed that mutations in *ZmWAK-RLK1* result in elevation of DIM_2BOA-Glc content. Compromising the synthesis of DIM_2BOA-Glc in Bx13NIL-Oh43 resulted in elevated NCLB resistance. The resistance caused by *ZmWAK-RLK1* is likely achieved via mediating a reduction of DIM_2BOA-Glc. Thus, the accumulative datasets suggest the functional divergence of BXD compounds (*e.g.* DIM_2BOA-Glc) in interaction with aphids, herbivores and fungal pathogens.

The biosynthesis pathway of BXDs starts with the formation of indole by conversion of indole-3-glycerol phosphate (Niemeyer, 2009). IGP and indole are secondary metabolites found cross kingdoms, and they can also stimulate the synthesis of auxin (*e.g.* the phytohormone indole-3-acetic acid, IAA) via tryptophan dependent and independent pathways (Woodward & Bartel, 2005). A former study found no difference of IAA content in the bx1 mutant compared to wild type (Maag *et al.*, 2016), suggesting that termination of the BXD pathway does not necessarily result in an increase of auxin biosynthesis. However, we cannot exclude at this stage that *Htn1* contributes to the modulation of the metabolic flux from IGP and/or indole into the BXD and IAA biosynthesis pathways. Thus, the reduced flux into the BXD pathway in the presence of *Htn1* could be accompanied by an increased flux into the auxin biosynthesis pathway, resulting in metabolic changes contributing to resistance.

The transcriptome data also revealed DEGs in several additional pathways related to immune responses. The presence of *Htn1*modifies the biosynthesis pathways of the defense hormones jasmonic acid and ethylene, lignin synthesis, cell wall strength and other receptor like kinases. For instance, >16 fold up-regulation of *OPR2* (9 hours post inoculation) and *LOX3* (before inoculation) were observed in w22Htn1 and B37Htn1 relative to the parental lines. Both genes are involved in the biosynthetic pathway of the phytohormone jasmonic acid that plays a central role in regulating resistance against hemibiotrophic and necrotrophic diseases (Glazebrook, 2005). JA treatment can induce the accumulation of BXD compounds (Oikawa *et al.*, 2001; Oikawa *et al.*, 2002). At this stage it remains unclear if there is a link between JAs, WAKs and BXDs metabolism. The gene *Caffeoyl-CoA O-methyltransferase 2* (*ZmCCoAOMT2*) is a key functional gene in lignin metabolic pathway and up-regulated (>5 fold) when *ZmWAK-RLK1* is present before pathogen inoculation. Recently, this gene

was shown to be associated with resistance against multiple foliage diseases including NCLB (Yang *et al.*, 2017), suggesting a link between *ZmWAK-RLK1*, lignin and NCLB resistance. Since about 50% of DEGs showed differential expression even before pathogen infection, this suggests a constitutive *ZmWAK-RLK1*-mediated immune response that might be expressed independently of the recognition of pathogen components (Jones & Dangl, 2006). Based on these data, we conclude that a number of metabolic pathways are modified in the presence of *Htn1* and it is possible that the observed resistance is the consequence of additive action of multiple biochemical changes in the plant.The transcriptome analysis revealed large number of DEGs in B37Htn1/B37 compared to w22Htn1/w22, but only a proportion of DEGs were shared. There implicated either *Htn1*-mediated resistance via different mechanisms in diverse genetic backgrounds, or most likely the presence of *Htn1*-unrelated un-specific DEGs caused by differences in genomic segments that are present in NILs.

In contrast to the Arabidopsis *WAK* gene family that consists of only five members, *WAK* genes in monocots belong to large families. For instance, in rice >100 members were found (Zhang *et al.*, 2005; Kanneganti & Gupta, 2008). A number of WAK genes in monocots have been shown to be associated to several functional aspects, e.g. biotic diseases (Li *et al.*, 2009; Hurni *et al.*, 2015; Zuo *et al.*, 2015; Shi *et al.*, 2016; Hu *et al.*, 2017), tolerance to phosphorus deficiency (Hufnagel *et al.*, 2014), root growth (Kaur *et al.*, 2013) as well as gametophyte development (Wang *et al.*, 2012). WAKs are the only known proteins that physically link the cell wall to the plasma membrane (Brutus *et al.*, 2010; Kohorn & Kohorn, 2012). They have been shown to be often associated with either of these two cell compartments (Brutus *et al.*, 2010; Wang *et al.*, 2012). ZmWAK-RLK1 is localized to the plasma membrane, very similar to the maize WAK protein ZmWAK/*qHSR1* that confers quantitative head smut disease resistance (Zuo *et al.*, 2015). ZmWAK-RLK1 can reduce pathogen penetration into host tissues and our transcriptome data revealed different expression levels of several cell wall related genes, suggesting a positive effect possibly in stabilization of the cell wall. This role has been demonstrated for the rice *OsWAK/Xa4* gene conferring quantitative rice blight resistance by strengthening the cell wall (Hu *et al.*, 2017). In contrast, the wheat WAK gene *TaWAK*/*Snn1* is hijacked by the necrotrophic effector SnTox1 that triggers programmed cell death allowing the pathogen to feed and grow on dead tissue (Shi *et al.*, 2016). Furthermore, these data show that elicitors recognized by WAKs can both be cell wall derived degraded polysaccharides (e.g. OGs) or pathogenic short peptides (SnTox1) (Brutus *et al.*, 2010; Shi *et al.*, 2016). Thus, although there is increasing evidence for a complex nature and functional divergence of WAKs in perception of types of ligands and in their role of interacting with biotic diseases, understanding the functional basis of WAKs is of interest to explore novel anti-fungal strategies relevant for a series of important crop plants such maize, rice and wheat.

Acknowledgements

The authors would like to thank Dr. Severine Hurni (UZH) for helpful discussions, Prof. Jiaqiang Sun (Institute of Crop Sciences, CAAS) for assistance in performance of western blot, Prof. Jianfeng Wen for assistance in performance of experiments with maize protoplasts, Prof. Georg Jander (Cornell University) for kindly providing *bx* mutants, and Mr. Alessandro Artemisio, Mr. Gerhard Herren, Mr. Karl Huwiler, Mr. Thibault Vassor and Ms. Matisse Petit-Prost for technical support. This work was supported by Swiss National Science Foundation Grant 310030_163260 to B. Keller. S.G.K. is supported by an Ambizione grant of the Swiss National Science Foundation. P.Y. is supported by Agricultural Science and Technology Innovation Program of CAAS and Fundamental Research Funds for Central Non-Profit of Institute of Crop Sciences of CAAS, China.

Contributions

P.Y., M.O., S.G.K., M.E. and B. Keller designed research; P.Y., C.P., B.L., J.S., C.R., B. Kessel, D.S. and L.L. performed research; P.Y., C.P., B.L., C.R., S.G.K., M.E. and B. Keller analyzed data; and P.Y., S.G.K., M.E., and B. Keller wrote the paper.

References

Ahmad S, Veyrat N, Gordon-Weeks R, Zhang YH, Martin J, Smart L, Glauser G, Erb M, Flors V, Frey M, Ton J. 2011. Benzoxazinoid metabolites regulate innate immunity against aphids and fungi in maize. *Plant Physiology* **157**(1): 317-327.

Balmer D, de Papajewski DV, Planchamp C, Glauser G, Mauch-Mani B. 2013. Induced resistance in maize is based on organ-specific defence responses. *Plant Journal* **74**(2): 213-225.

Brutus A, Sicilia F, Macone A, Cervone F, De Lorenzo G. 2010. A domain swap approach reveals a role of the plant wall-associated kinase 1 (WAK1) as a receptor of oligogalacturonides. *Proceedings of the National Academy of Sciences of the United States of America* **107**(20): 9452-9457.

Ceballos H, Gracen VE. 1989. A dominant inhibitor gene inhibits the expression of *Ht2* against *Exserohilum turcicum* race 2 in corn inbred lines related to B14. *Plant Breeding* **102**: 35-44.

Chung CL, Jamann T, Longfellow J, Nelson R. 2010. Characterization and fine-mapping of a resistance locus for northern leaf blight in maize bin 8.06. *Theoretical and Applied Genetics* **121**(2): 205-227.

Couture RM, Routley DG, Dunn GM. 1971. Role of cyclic hydroxamic acids in monogenic resistance of maize to *Helminthosporium turcicum*. *Physiological Plant Pathology* **1**(4): 515-521.

Dardick C, Schwessinger B, Ronald P. 2012. Non-arginine-aspartate (non-RD) kinases are associated with innate immune receptors that recognize conserved microbial signatures. *Current Opinion in Plant Biology* **15**(4): 358-366.

Decreux A, Thomas A, Spies B, Brasseur R, Van Cutsem P, Messiaen J. 2006. In vitro characterization of the homogalacturonan-binding domain of the wall-associated kinase WAK1 using site-directed mutagenesis. *Phytochemistry* **67**(11): 1068-1079.

Di DW, Zhang C, Luo P, An CW, Guo GQ. 2016. The biosynthesis of auxin: how many paths truly lead to IAA? *Plant Growth Regulation* **78**(3): 275-285.

Dobin A, Davis CA, Schlesinger F, Drenkow J, Zaleski C, Jha S, Batut P, Chaisson M, Gingeras TR. 2013. STAR: ultrafast universal RNA-seq aligner. *Bioinformatics* **29**(1): 15-21.

Du Z, Zhou X, Ling Y, Zhang ZH, Su Z. 2010. agriGO: a GO analysis toolkit for the agricultural community. *Nucleic Acids Research* **38**: W64-W70.
Elnaghy M, Pekka L. 1962. The role of 4-o-glueosyl-2,4-dihydroxy-7-methoxy-l,4-benzoxazin-3-one resistance of wheat to stem rust. *Pysiologia Plantarum* **15**: 764-771.
Erb M, Robert CAM, Hibbard BE, Turlings TCJ. 2011. Sequence of arrival determines plant-mediated interactions between herbivores. *Journal of Ecology* **99**(1): 7-15.
Frey M, Stettner C, Pare PW, Schmelz EA, Tumlinson JH, Gierl A. 2000. An herbivore elicitor activates the gene for indole emission in maize. *Proceedings of the National Academy of Sciences of the United States of America* **97**(26): 14801-14806.
Glazebrook J. 2005. Contrasting mechanisms of defense against biotrophic and necrotrophic pathogens. *Annual review of phytopathology* **43**: 205-227.
Gomez-Gomez L, Boller T. 2000. FLS2: An LRR receptor-like kinase involved in the perception of the bacterial elicitor flagellin in Arabidopsis. *Molecular Cell* **5**(6): 1003-1011.
Grefen C, Donald N, Hashimoto K, Kudla J, Schumacher K, Blatt MR. 2010. A ubiquitin-10 promoter-based vector set for fluorescent protein tagging facilitates temporal stability and native protein distribution in transient and stable expression studies. *Plant Journal* **64**(2): 355-365.
Handrick V, Robert CAM, Ahern KR, Zhou SQ, Machado RAR, Maag D, Glauser G, Fernandez-Penny FE, Chandran JN, Rodgers-Melnik E, Schneider B, Buckler ES, Boland W, Gershenzon J, Jander G, Erb M, Kollner TG. 2016. Biosynthesis of 8-o-methylated benzoxazinoid defense compounds in maize. *Plant Cell* **28**(7): 1682-1700.
Hilu HM, Hooker AL. 1964. localized infection by *helminthosporium turcicum* on cron leaves. *Phytopathology* **55**: 189-192.
Houseman JG, Campos F, Thie NMR, Philogène BJR, Atkinson J, Morand P, Arnason JT. 1992. Effect of the maize-derived compounds DIMBOA and MBOA on growth and digestive processes of European corn borer (Lepidoptera: *Pyralidae*) *Journal of Economic Entomology* **85**(3): 6.
Hu KM, Cao JB, Zhang J, Xia F, Ke YG, Zhang HT, Xie WY, Liu HB, Cui Y, Cao YL, Sun XL, Xiao JH, Li XH, Zhang QL, Wang SP. 2017. Improvement of multiple agronomic traits by a disease resistance gene via cell wall reinforcement. *Nature Plants* **3**(3): 17009.
Hufnagel B, de Sousa SM, Assis L, Guimaraes CT, Leiser W, Azevedo GC, Negri B, Larson BG, Shaff JE, Pastina MM, Barros BA, Weltzien E, Frederick H, Rattunde W, Viana JH, Clark RT, Falcao A, Gazaffi R, Garcia AAF, Schaffert RE, Kochian LV, Magalhaes JV. 2014. Duplicate and conquer: multiple homologs of *PHOSPHORUS-STARVATION TOLERANCE1* enhance phosphorus acquisition and sorghum performance on Low-phosphorus soils. *Plant Physiology* **166**(2): 659-677.
Hurni S, Scheuermann D, Krattinger SG, Kessel B, Wicker T, Herren G, Fitze MN, Breen J, Presterl T, Ouzunova M, Keller B. 2015. The maize disease resistance gene *Htn1* against northern corn leaf blight encodes a wall-associated receptor-like kinase. *Proceedings of the National Academy of Sciences of the United States of America* **112**(28): 8780-8785.
Jennings PR, Ullstrup AJ. 1957. A histological study of three *Helminthosporium* leaf blights of corn. *Phytopathology* **47**: 707-714.
Jones JDG, Dangl JL. 2006. The plant immune system. *Nature* **444**(7117): 323-329.
Kanneganti V, Gupta AK. 2008. Wall associated kinases from plants - an overview. *Physiol Mol Biol Plants* **14**(1-2): 109-118.
Kaur R, Singh K, Singh J. 2013. A root-specific wall-associated kinase gene, *HvWAK1*, regulates root growth and is highly divergent in barley and other cereals. *Functional & Integrative Genomics* **13**(2): 167-177.
Kohler A, Maag D, Veyrat N, Glauser G, Wolfender JL, Turlings TCJ, Erb M. 2015. Within-plant distribution of 1,4-benzoxazin-3-ones contributes to herbivore niche differentiation in maize. *Plant Cell and Environment* **38**(6): 1081-1093.
Kohorn BD, Kohorn SL. 2012. The cell wall-associated kinases,WAKs, as pectin receptors. *Front Plant Sci* **3**: 88.
Kostandi SF, Koraiem YS, Kamara A, Omar MA. 1981. Effect of phenols in host-pathogen: interaction of maize (*Zea mays* L.). *Cephalosporium maydis* system. *Agrochimica* **25**(3-4): 367-375.

Krattinger SG, Keller B. 2016. Molecular genetics and evolution of disease resistance in cereals. *New Phytologist* **212**(2): 320-332.
Li H, Zhou SY, Zhao WS, Su SC, Peng YL. 2009. A novel wall-associated receptor-like protein kinase gene, *OsWAK1*, plays important roles in rice blast disease resistance. *Plant Molecular Biology* **69**(3): 337-346.
Liao Y, Smyth GK, Shi W. 2014. featureCounts: an efficient general purpose program for assigning sequence reads to genomic features. *Bioinformatics* **30**(7): 923-930.
Long BJ, Dunn GM, Routley DG. 1978. Relationship of hydroxamate concentration in maize and field reaction to *Helminthosporium turcicum*. *Crop Sci* **18**(4): 573-575.
Maag D, Kohler A, Robert CAM, Frey M, Wolfender JL, Turlings TCJ, Glauser G, Erb M. 2016. Highly localized and persistent induction of Bx1-dependent herbivore resistance factors in maize. *Plant Journal* **88**(6): 976-991.
Macho AP, Zipfel C. 2014. Plant PRRs and the activation of innate immune signaling. *Molecular Cell* **54**(2): 263-272.
Meihls LN, Handrick V, Glauser G, Barbier H, Kaur H, Haribal MM, Lipka AE, Gershenzon J, Buckler ES, Erb M, Kollner TG, Jander G. 2013. Natural variation in maize aphid resistance is associated with 2,4-dihydroxy-7-methoxy-1,4-benzoxazin-3-one glucoside methyltransferase activity. *Plant Cell* **25**(6): 2341-2355.
Nelson BK, Cai X, Nebenfuhr A. 2007. A multicolored set of in vivo organelle markers for co-localization studies in Arabidopsis and other plants. *Plant Journal* **51**(6): 1126-1136.
Niemeyer HM. 2009. Hydroxamic acids derived from 2-hydroxy-2H-1,4-benzoxazin-3(4H)-one: key defense chemicals of cereals. *Journal of Agricultural and Food Chemistry* **57**(5): 1677-1696.
Oikawa A, Ishihara A, Hasegawa M, Kodama O, Iwamura H. 2001. Induced accumulation of 2-hydroxy-4,7-dimethoxy-1,4-benzoxazin-3-one glucoside (HDMBOA-Glc) in maize leaves. *Phytochemistry* **56**(7): 669-675.
Oikawa A, Ishihara A, Iwamura H. 2002. Induction of HDMBOA-Glc accumulation and DIMBOA-Glc 4-O-methyltransferase by jasmonic acid in poaceous plants. *Phytochemistry* **61**(3): 331-337.
Oikawa A, Ishihara A, Tanaka C, Mori N, Tsuda M, Iwamura H. 2004. Accumulation of HDMBOA-Glc is induced by biotic stresses prior to the release of MBOA in maize leaves. *Phytochemistry* 65(22): 2995-3001.
Raymundo AD, Hooker AL, Perkins JM. 1981. Effect of gene *HtN* on the development of northern corn leaf blight epidemics. *Plant Disease* **65**(4): 327-330.
Robert CAM, Veyrat N, Glauser G, Marti G, Doyen GR, Villard N, Gaillard MDP, Kollner TG, Giron D, Body M, Babst BA, Ferrieri RA, Turlings TCJ, Erb M. 2012. A specialist root herbivore exploits defensive metabolites to locate nutritious tissues. *Ecology Letters* **15**(1): 55-64.
Robinson MD, McCarthy DJ, Smyth GK. 2010. edgeR: a Bioconductor package for differential expression analysis of digital gene expression data. *Bioinformatics* **26**(1): 139-140.
Shi G, Zhang Z, Friesen TL, Raats D, Fahima T, Brueggeman RS, Lu S, Trick HN, Liu Z, Chao W, Frenkel Z, Xu SS, Rasmussen JB, Faris JD. 2016. The hijacking of a receptor kinase-driven pathway by a wheat fungal pathogen leads to disease. *Science Advances* **2**(10): e1600822.
Song YY, Cao M, Xie LJ, Liang XT, Zeng RS, Su YJ, Huang JH, Wang RL, Luo SM. 2011. Induction of DIMBOA accumulation and systemic defense responses as a mechanism of enhanced resistance of mycorrhizal corn (*Zea mays* L.) to sheath blight. *Mycorrhiza* **21**(8): 721-731.
Vollbrecht E, Duvick J, Schares JP, Ahern KR, Deewatthanawong P, Xu L, Conrad LJ, Kikuchi K, Kubinec TA, Hall BD, Weeks R, Unger-Wallace E, Muszynski M, Brendel VP, Brutnell TP. 2010. Genome-wide distribution of transposed dissociation elements in maize. *Plant Cell* **22**(6): 1667-1685.
Wang N, Huang HJ, Ren ST, Li JJ, Sun Y, Sun DY, Zhang SQ. 2012. The rice wall-associated receptor-like kinase gene *OsDEES1* plays a role in female gametophyte development. *Plant Physiology* **160**(2): 696-707.
Welz HG, Geiger HH. 2000. Genes for resistance to northern corn leaf blight in diverse maize populations. *Plant Breeding* **119**(1): 1-14.

606 **Woodward AW, Bartel B. 2005.** Auxin: regulation, action, and interaction. *Annals of Botany* **95**(5):
607 707-735.
608 **Wouters FC, Blanchette B, Gershenzon J, Vassao DG. 2016.** Plant defense and herbivore counter-
609 defense: benzoxazinoids and insect herbivores. *Phytochemistry Reviews* **15**(6): 1127-
610 1151.**Yang P, Herren G, Krattinger SG, Keller B. 2017.** Large-scale maize seedling infection
611 with *Exserohilum turcicum* in the greenhouse. *Bio-protocol* **7**(19): e2567.
612 **Yang Q, He Y, Kabahuma M, Chaya T, Kelly A, Borrego E, Bian Y, El Kasmi F, Yang L, Teixeira P,**
613 **Kolkman J, Nelson R, Kolomiets M, J LD, Wisser R, Caplan J, Li X, Lauter N, Balint-Kurti P.**
614 **2017.** A gene encoding maize caffeoyl-CoA O-methyltransferase confers quantitative
615 resistance to multiple pathogens. *Nature Genetics* **49**(9): 1364-1372.
616 **Yoo SD, Cho YH, Sheen J. 2007.** Arabidopsis mesophyll protoplasts: a versatile cell system for
617 transient gene expression analysis. *Nature Protocols* **2**(7): 1565-1572.
618 **Zhang SB, Chen C, Li L, Meng L, Singh J, Jiang N, Deng XW, He ZH, Lemaux PG. 2005.** Evolutionary
619 expansion, gene structure, and expression of the rice wall-associated kinase gene family.
620 *Plant Physiology* **139**(3): 1107-1124.
621 **Zipfel C, Oldroyd GED. 2017.** Plant signalling in symbiosis and immunity. *Nature* **543**(7645): 328-336.
622 **Zuo WL, Chao Q, Zhang N, Ye JR, Tan GQ, Li BL, Xing YX, Zhang BQ, Liu HJ, Fengler KA, Zhao J, Zhao**
623 **XR, Chen YS, Lai JS, Yan JB, Xu ML. 2015.** A maize wall-associated kinase confers quantitative
624 resistance to head smut. *Nature Genetics* **47**(2): 151-157.

625

626 **Figure legends**

627 **Fig. 1 ZmWAK-RLK1 localizes to the plasma membrane in maize**. (A-B) Fluorescent signals in onion
628 epidermal cells after transient expression of ZmWAK-RKL1-eGFP and the positive control PIP2A-
629 mCherry that is known to localize to the plasma membrane (Kammerloher et al. 1994; Nelson et al.
630 2007). Signals are shown before (A) and after (B) plasmolysis with 0.8 mol/L (M) mannitol. (C)
631 Fluorescent signals in *N. benthamiana* leaves two days after infiltration. (D) Fluorescent signals in
632 maize protoplasts 36 hours after transformation. Scale bars, 50µm.

633 **Fig. 2 *ZmWAK-RLK1* reduced the fungal penetration rates in the seedling leaves of maize**. (A)
634 Hyphae detected inside of host tissues at 1 dpi. In the left and right panels the focus is on the
635 epidermis and hyphae, respectively. The red arrows indicate the hyphae inside the host tissue. Scale
636 bars, 100µm. (B) Rate of successful penetration events at 1 dpi. The genotypes RLK1b, RLK1d and
637 RLK1f are *ZmWAK-RLK1* mutants with compromised northern corn leaf blight (NCLB) resistance that
638 were produced in RP3Htn1 (Hurni et al. 2015), while genotypes RLK1b-wt, RLK1d-wt and RLK1f-wt
639 are the corresponding sister lines, respectively. Red bar, *Htn1* resistance allele; black bar, susceptible
640 allele. The statistical analysis was conducted using Student's t test in three independent experiments.
641 The asterisks represent a significant difference of $^{**}p<0.01$ or $^{*}p<0.05$. (C) Rate of successful
642 penetration events at 3 dpi in B37 and B37Htn1. The statistical analysis was conducted using Tukey's
643 HSD in three biological replicates. The lowercase letters represent the significant difference ($p = 0.05$).
644 Error bars indicate ± standard error (SE).

Fig. 3 Content of BXDs in maize genotypes w22 and w22Htn1. (A) The proposed biosynthesis pathway of benzoxazinoid (BXD) secondary metabolites. The genes that catalyze each step of enzymatic reactions are given. The contents of BXD compounds DIMBOA-Glc (B), DIMBOA (C), HMBOA-Glc (D), DIM_2BOA-Glc (E) and HDMBOA-Glc (F) were determined before inoculation, at 3 dpi and 10 dpi. TRIMBOA-Glc and HDM_2BOA-Glc are below than the detection limit and not shown. The statistical analysis was conducted using Tukey's HSD (P = 0.05) in eight biological replicates. The lowercase letters represent the significant difference (p = 0.05). Error bars are ± SE.

Fig. 4 Mutations in BXDs biosynthesis genes increased resistance to NCLB disease at the seedling stage of maize. (A) Visual symptoms and (B) quantified NCLB disease severity in *bx* mutants in the w22 genetic background. (C) Expression of *ZmWAK-RLK1* at 10 dpi. Statistical analysis was conducted using Student's t test. The asterisks represent a significant difference of $^{**}p$<0.01 or $^{*}p$<0.05. ns: no significance (p = 0.05). Error bars are ± SE.

Fig. 5 A knockout mutation of the *Bx13* gene increases NCLB resistance of maize. Bx13NIL-B73 contains a wild type functional *Bx13* allele and Bx13NIL-Oh43 contains a non-functional *bx13* allele, which results in the elimination of DIM_2BOA-Glc (Hardick et al. 2016). The statistical analysis was conducted using Student's t test (n=45). PrimDLA, the primary diseased leaf area of the inoculated leaves. The asterisks represent a significant difference of $^{**}p$<0.01 or $^{*}p$<0.05. ns: no significance (p = 0.05). Error bars are ± SE.

Fig. 6 Mutations in *ZmWAK-RLK1* result in elevated DIM_2BOA-Glc content that is associated with *Igl* expression in maize. (A) Content of DIM_2BOA-Glc in mutants and corresponding sister lines before infection at 21 days after sowing (n=8). (B) Expression analysis of *Igl* (n=5). The statistical analysis was conducted using Student's t test. The asterisks represent a significant difference of $^{**}p$<0.01 or $^{*}p$<0.05. Error bars are ± SE.

Supporting information

Table S1 Information of the maize genotypes with and without *Htn1* used in different experiments of this study

Table S2 Setup of RT-qPCR assays for target genes

Table S3 Statistics of RNA-seq reads sequenced and mapped

Table S4 The logFC and annotation of 215 differently expressed genes (see separate Excel file)

Fig. S1 Western blotting analysis of the fusion protein of ZmWAK-RLK1 and GFP.

Fig. S2 Quantitative analysis of the infection steps of *E. turcicum* in maize seedlings at 1 dpi.

Fig. S3 Disease phenotype of NILs with and without *Htn1*

Fig. S4 Multidimensional scaling (MDS) analysis in RNAseq datasets using normalized expression by edgeR

Fig. S5 Transcriptome analysis in NILs with and without *Htn1* revealed a set of DEGs

Fig. S6 Gene Ontology analysis for 215 DEGs

Fig. S7 Expression levels of *ZmWAK-RLK1* and BXD synthesis genes in w22 and w22Htn1

Fig. S8 Infection of *S. littoralis* and *D. balteata* in w22 and w22Htn1

Fig. S9 Content of BXD compounds in the second leaves of bx mutants at 10 dpi

Fig. S10 Content of BXD compounds in the second leaves of *Htn1* NILs and mutants at 21 days after sowing

Fig. S11 Expression levels of *ZmWAK-RLK1* and BXD synthesis genes in the second leaves of *Htn1* NILs and mutants at 21 days after sowing

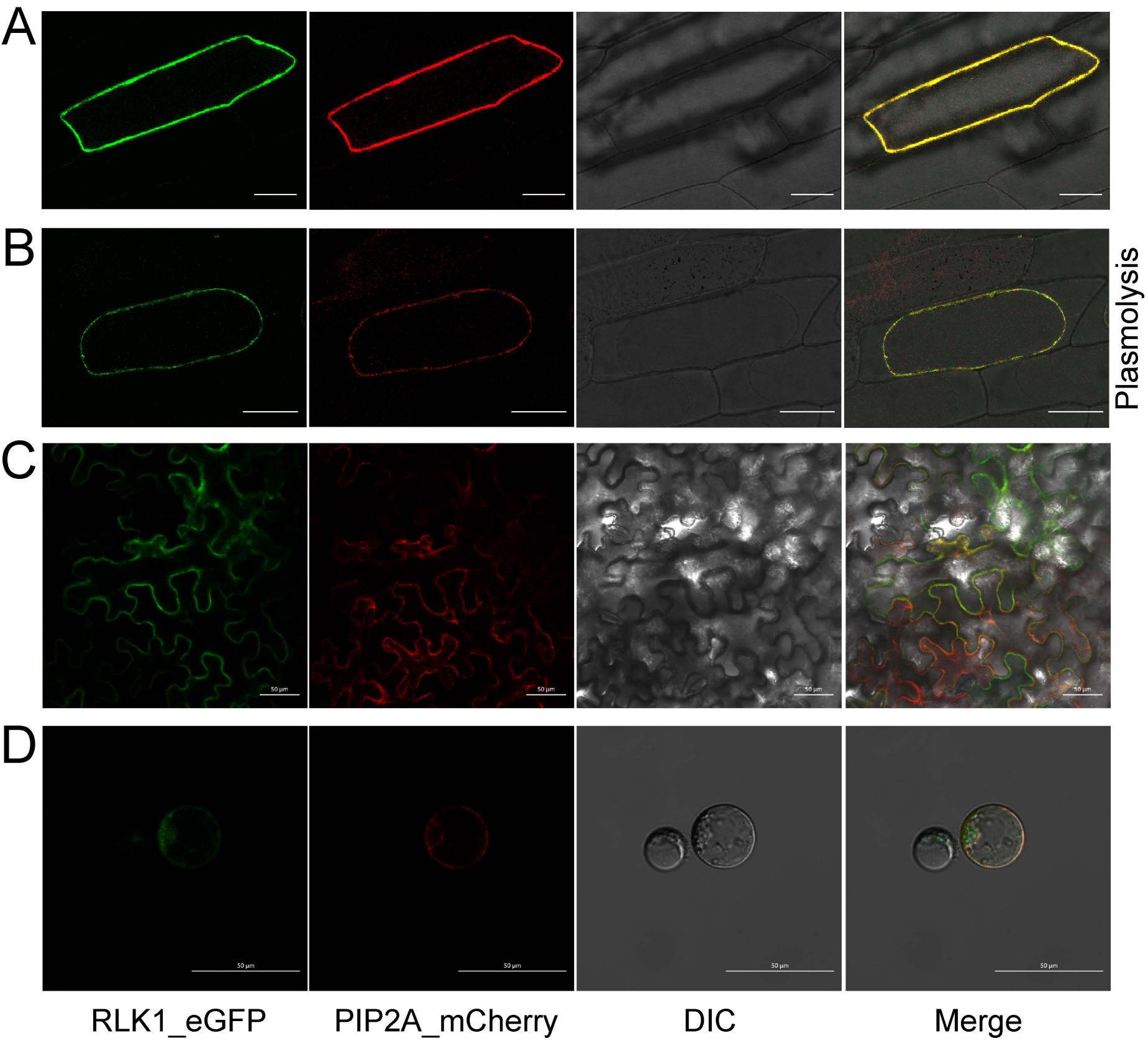
A
B
C
D
Plasmolysis
50 µm
RLK1_eGFP
PIP2A_mCherry
DIC
Merge

A

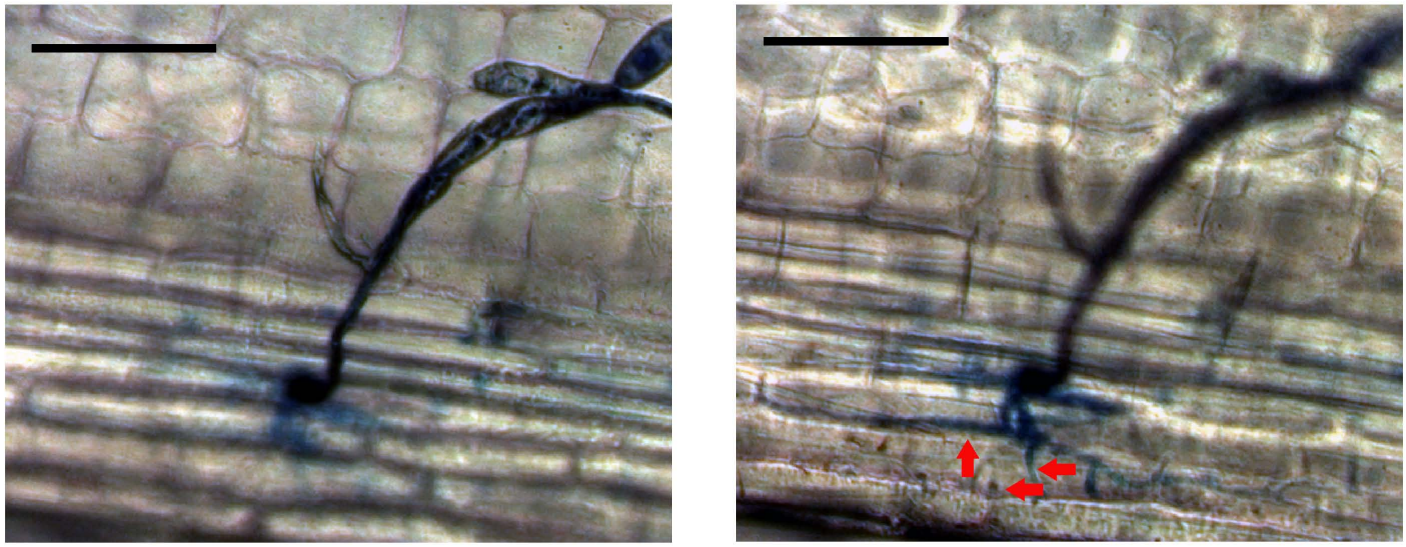

B

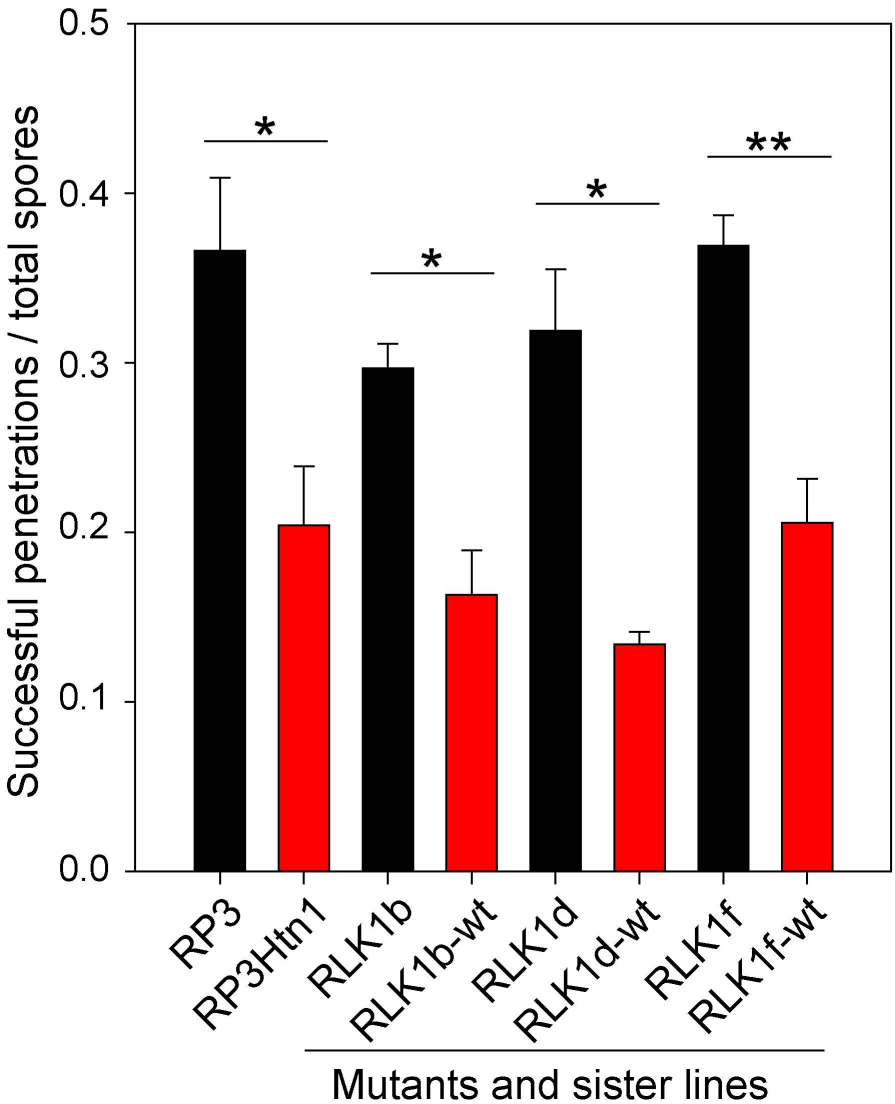
Successful penetrations / total spores
0.0
0.1
0.2
0.3
0.4
0.5
*
*
*
**
RP3
RP3Htn1
RLK1b
RLK1b-wt
RLK1d
RLK1d-wt
RLK1f
RLK1f-wt
Mutants and sister lines

C

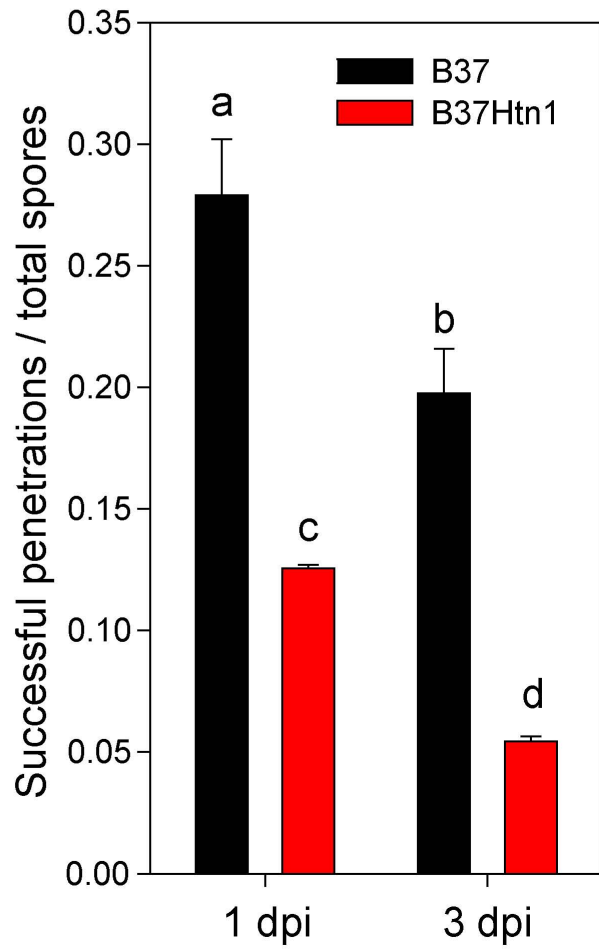
Successful penetrations / total spores
0.00
0.05
0.10
0.15
0.20
0.25
0.30
0.35
B37
B37Htn1
a
b
c
d
1 dpi
3 dpi

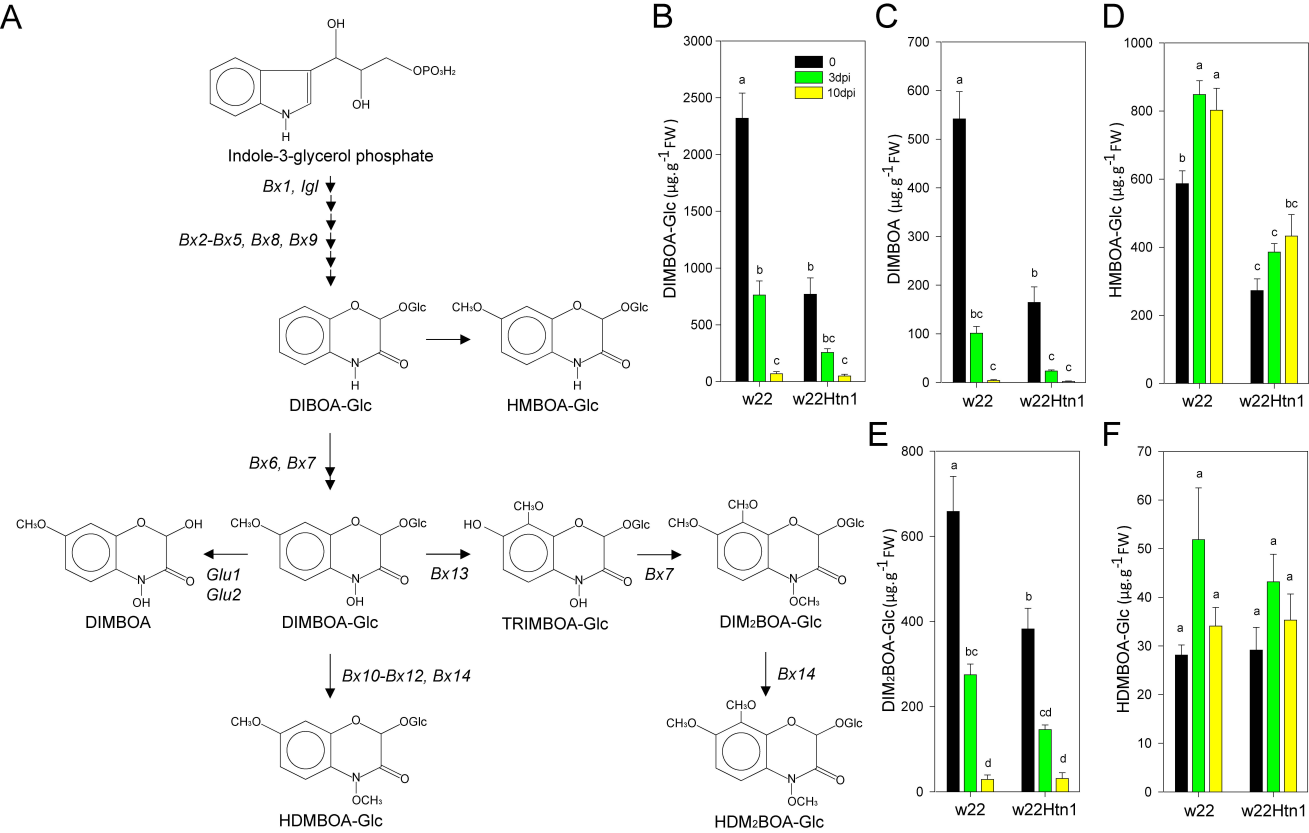
A
Indole-3-glycerol phosphate
Bx1, Igl
Bx2-Bx5, Bx8, Bx9
DIBOA-Glc
HMBOA-Glc
Bx6, Bx7
DIMBOA
DIMBOA-Glc
TRIMBOA-Glc
DIM2BOA-Glc
Glu1
Glu2
Bx13
Bx7
Bx10-Bx12, Bx14
Bx14
HDMBOA-Glc
HDM2BOA-Glc
B
DIMBOA-Glc (μg.g-1FW)
0
3dpi
10dpi
w22
w22Htn1
C
DIMBOA (μg.g-1FW)
D
HMBOA-Glc (μg.g-1FW)
E
DIM2BOA-Glc (μg.g-1FW)
F
HDMBOA-Glc (μg.g-1FW)

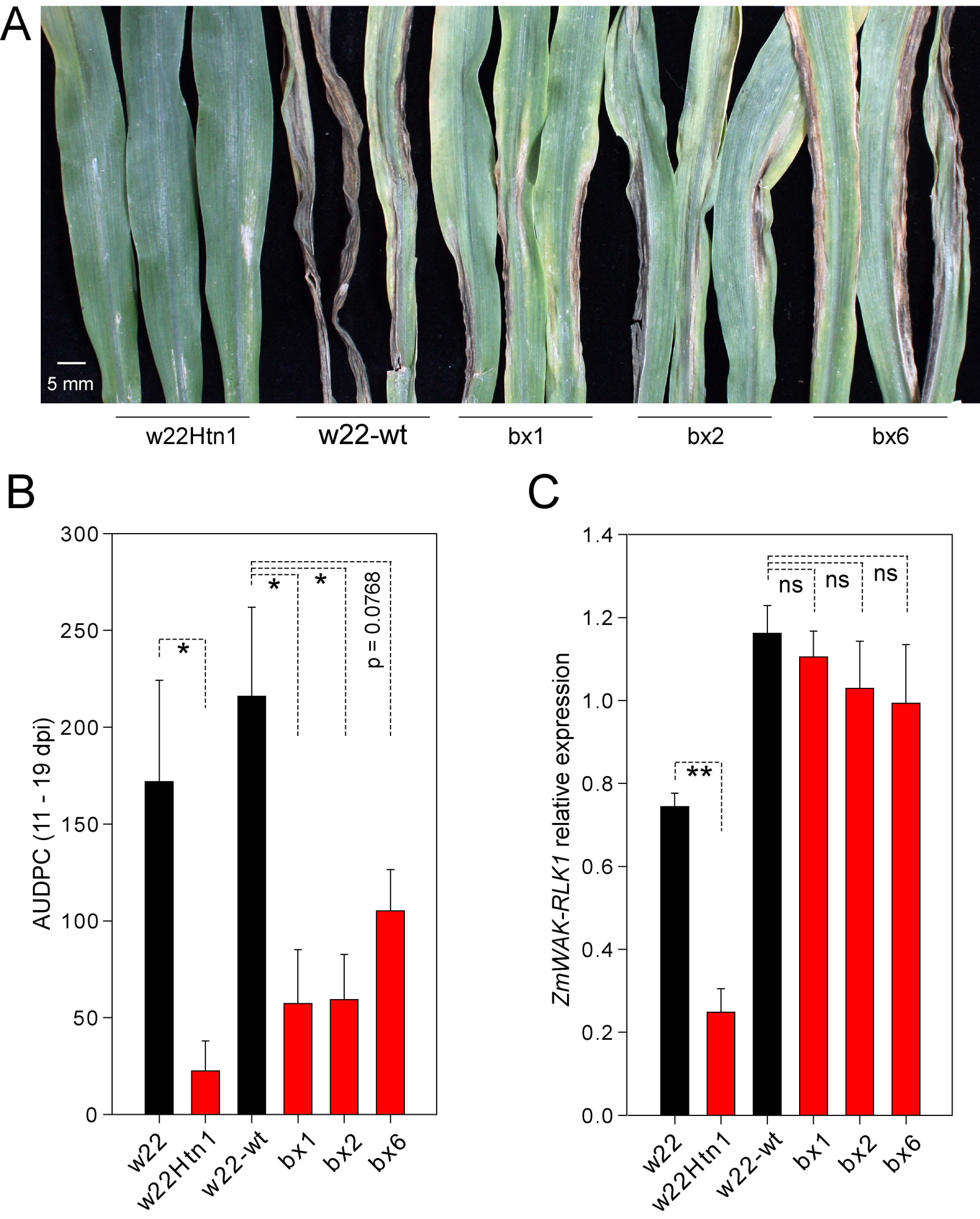
A
5 mm
w22Htn1
w22-wt
bx1
bx2
bx6
B
AUDPC (11 - 19 dpi)
300
250
200
150
100
50
0
*
*
*
p = 0.0768
w22
w22Htn1
w22-wt
bx1
bx2
bx6
C
ZmWAK-RLK1 relative expression
1.4
1.2
1.0
0.8
0.6
0.4
0.2
0.0
**
ns
ns
ns
w22
w22Htn1
w22-wt
bx1
bx2
bx6

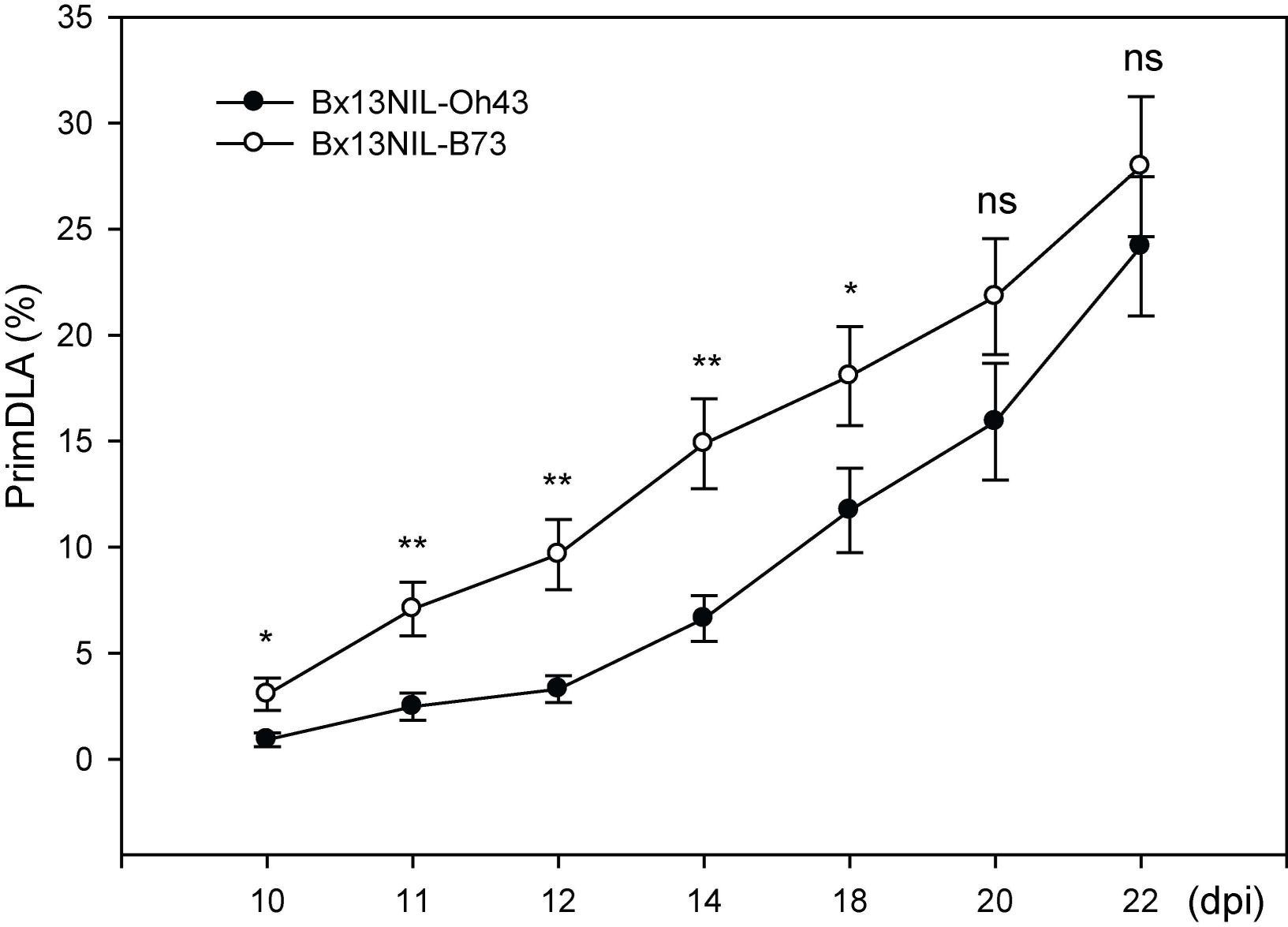
Bx13NIL-Oh43
Bx13NIL-B73
PrimDLA (%)
35
30
25
20
15
10
5
0
10
11
12
14
18
20
22
(dpi)
*
**
**
**
*
ns
ns

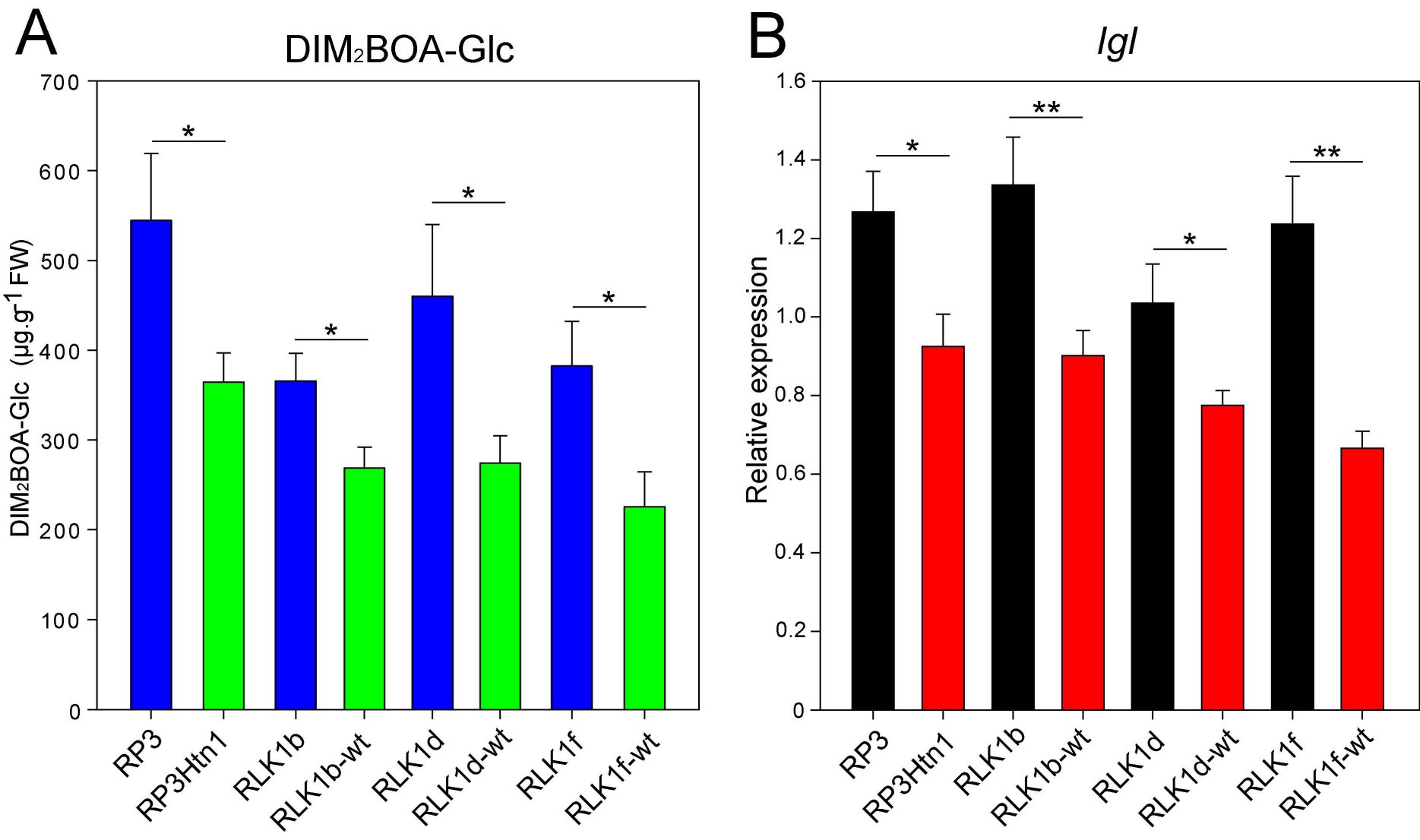
A
DIM2BOA-Glc
DIM2BOA-Glc (µg.gr-1 FW)
700
600
500
400
300
200
100
0
*
*
*
*
RP3
RP3Htn1
RLK1b
RLK1b-wt
RLK1d
RLK1d-wt
RLK1f
RLK1f-wt
B
lgl
Relative expression
1.6
1.4
1.2
1.0
0.8
0.6
0.4
0.2
0
*
**
*
**
RP3
RP3Htn1
RLK1b
RLK1b-wt
RLK1d
RLK1d-wt
RLK1f
RLK1f-wt

***New Phytologist* Supporting Information**

Article title: Fungal resistance mediated by maize wall-associated kinase ZmWAK-RLK1 correlates with reduced benzoxazinoid content

Authors: Ping Yang[1,4], Coraline Praz[1], Beibei Li[2], Jyoti Singla[1], Christelle Robert[2], Bettina Kessel[3], Daniela Scheuermann[3], Linda Lüthi[1], Milena Ouzunova[3], Matthias Erb[2*], Simon G. Krattinger[1,5*], Beat Keller[1*]

Article acceptance date: 30 July 2018

The following Supporting Information is available for this article:

Fig. S1 Western blotting analysis of the fusion protein of ZmWAK-RLK1 and GFP

Fig. S1 Western blotting analysis of the fusion protein of ZmWAK-RLK1 and GFP. Total protein was subjected for western blotting using anti-GFP-antibody.

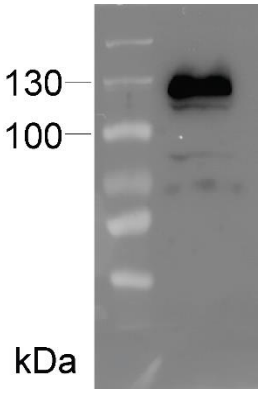

Fig. S2 Quantitative analysis of the infection steps of *E. turcicum* in maize seedlings at 1 dpi

Fig. S2 Quantitative analysis of the infection steps of *E. turcicum* in maize seedlings at 1 dpi. (A) Micrograph of a germinated spore and appressorium. (B) Penetration peg. (C) Hyphae in epidermal cells. (D) Number of germ tubes per spore. (E) Number of appressoria per spore. The numbers of counted spores in each experiment are given. The statistical analysis was conducted using Student's t test, based on the results of three independent experiments. ns: no significance ($p = 0.05$). Error bars are ± SE. Scale bars, 100μm.

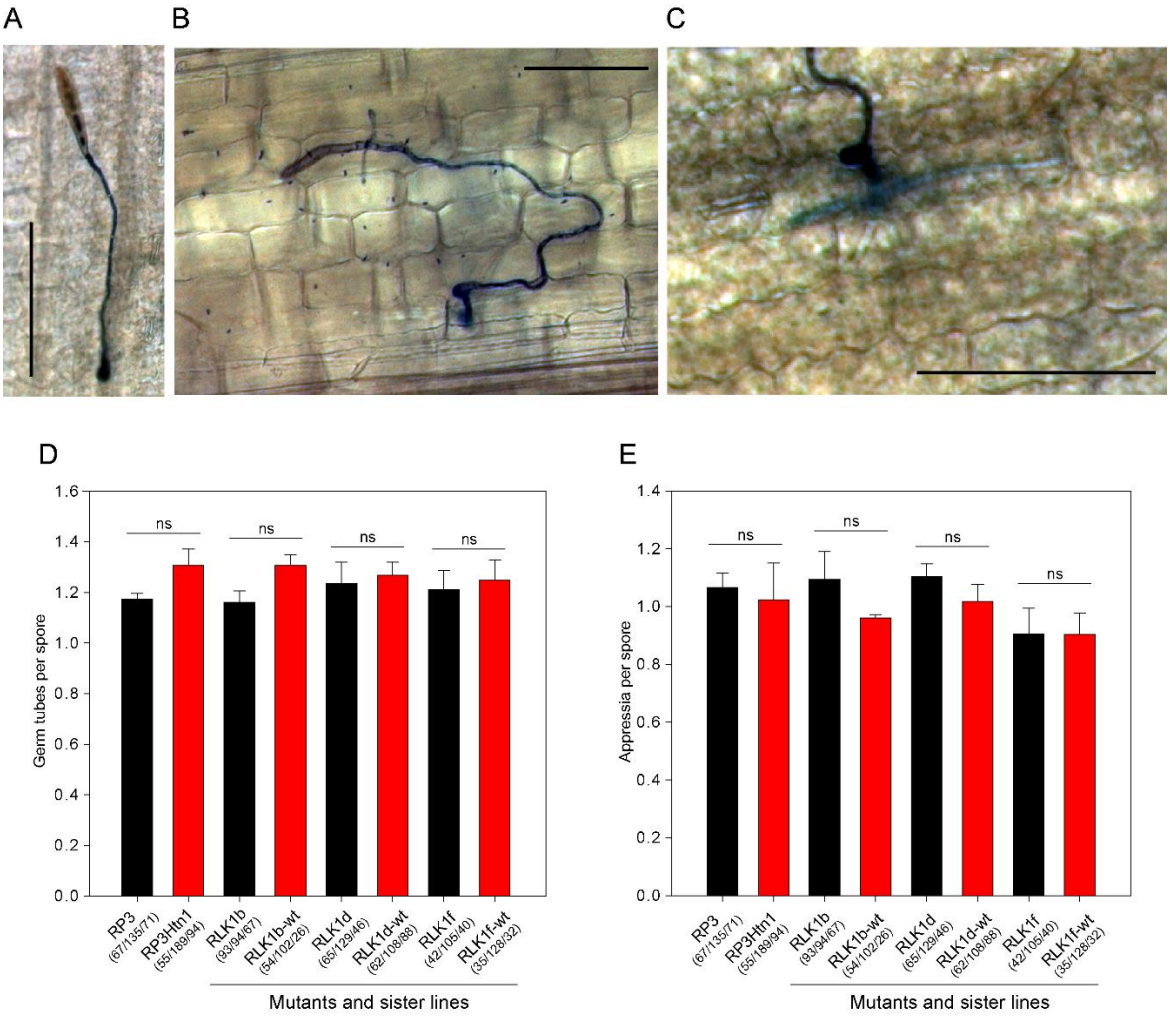

Fig. S3 Disease phenotype of NILs with and without *Htn1*

Fig. S3 Disease phenotype of NILs with and without *Htn1*. (A) Disease symptoms of the second leaves at 16 dpi. (B) Rate of infected plants. (C) Area under the disease progress curve (AUDPC). *AUDPC in this panel was calculated as described in Hurni et al. 2015, based on calculating the sum of the rate of infected plants (%).

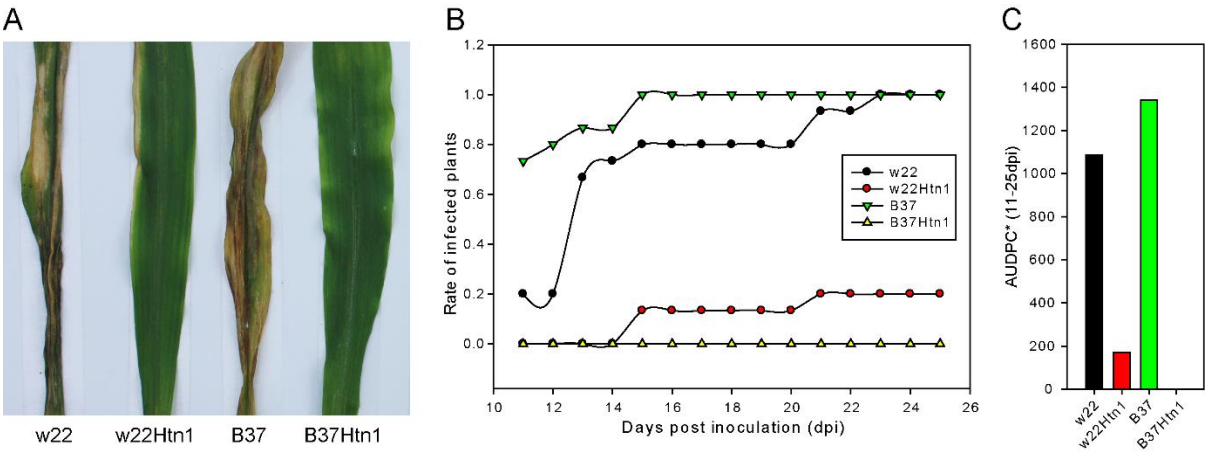

Fig. S4 Multidimensional scaling (MDS) analysis in RNAseq datasets using normalized expression by edgeR

Fig. S4 Multidimensional scaling (MDS) analysis in RNAseq datasets using normalized expression by edgeR (Robinson et al., 2010). Each symbol indicates one genotype-time point combined sample. (A) MDS plot of two pairs of NILs and the corresponding parental lines. (B) MDS plot of B37 and B37Htn1. (C) MDS plot of w22 and w22Htn1.

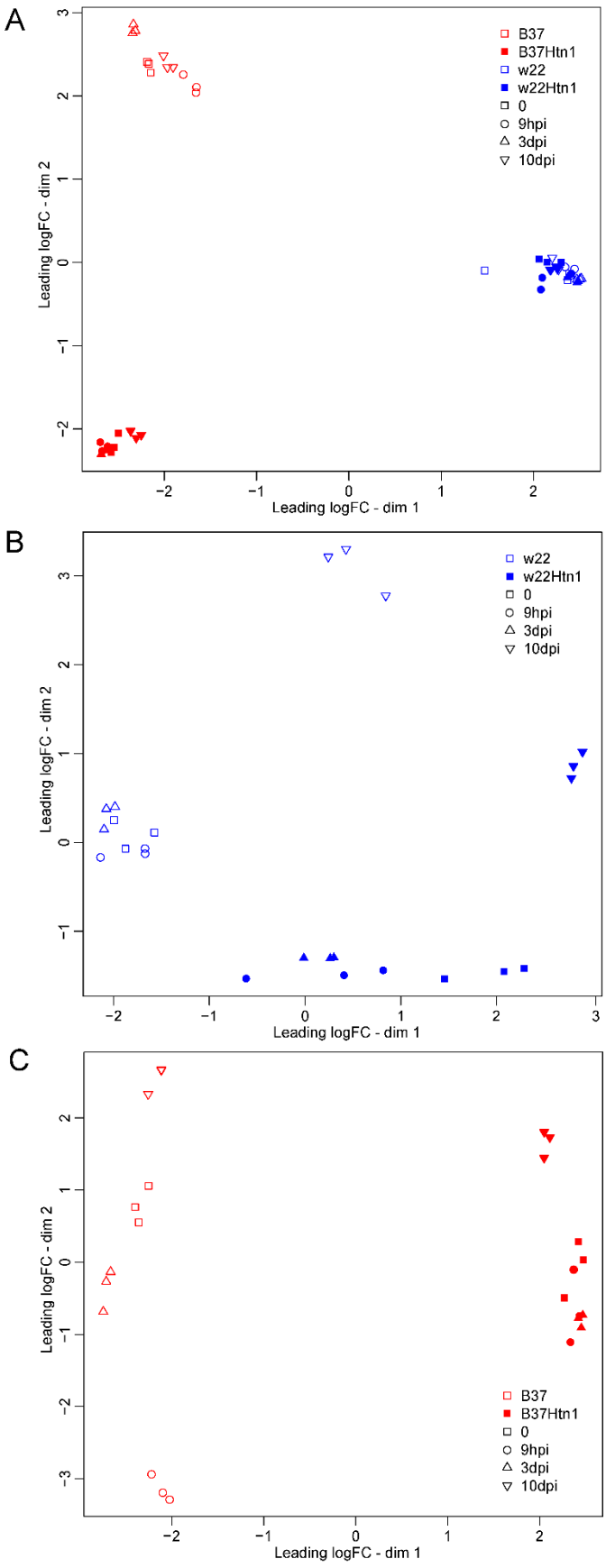
A
B37
B37Htn1
w22
w22Htn1
0
9hpi
3dpi
10dpi
Leading logFC - dim 2
Leading logFC - dim 1
B
w22
w22Htn1
0
9hpi
3dpi
10dpi
Leading logFC - dim 2
Leading logFC - dim 1
C
B37
B37Htn1
0
9hpi
3dpi
10dpi
Leading logFC - dim 2
Leading logFC - dim 1

Fig. S5 Transcriptome analysis in NILs with and without *Htn1* revealed a set of DEGs

Fig. S5 Transcriptome analysis in NILs with and without *Htn1* revealed a set of DEGs. (A) Number of DEGs in the two *Htn1* NILs compared to the parental lines without *Htn1*. (B) Clustering of 215 DEGs shared in comparisons of both NILs w22Htn1/w22 and B37Htn1/B37. These genes were differentially expressed in both NILs in at least one of time points. The colors of the heat map correspond to logFC (fold change). (C) Venn diagram representing the number of shared DEGs at the different time points.

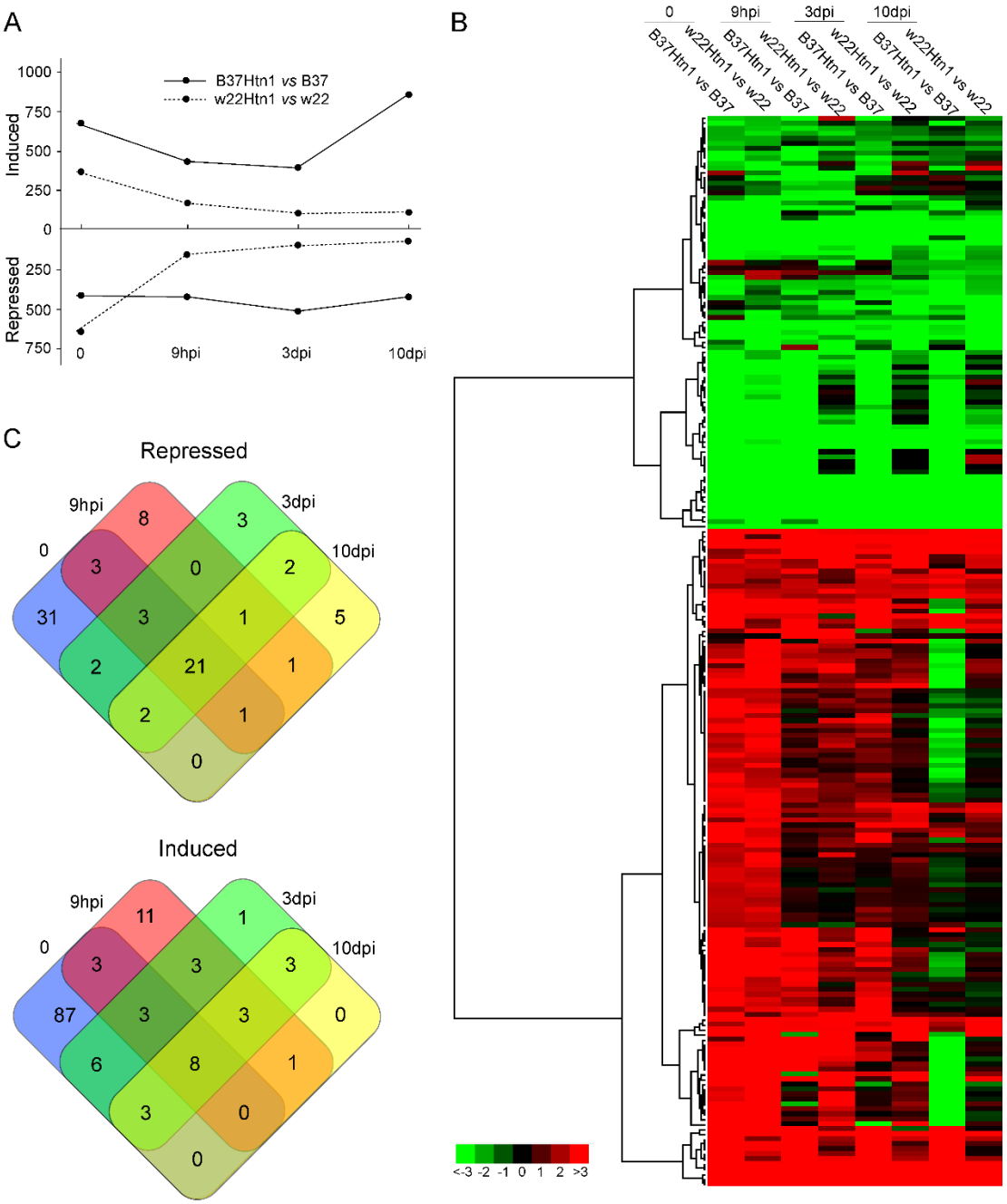

Fig. S6 Gene Ontology analysis for 215 DEGs

Fig. S6 Gene Ontology analysis for 215 DEGs. The Gene Ontology analysis was conducted by using online software agriGO (Du et al. 2010). The significant terms were colored if adjusted $p \leqslant 0.05$.

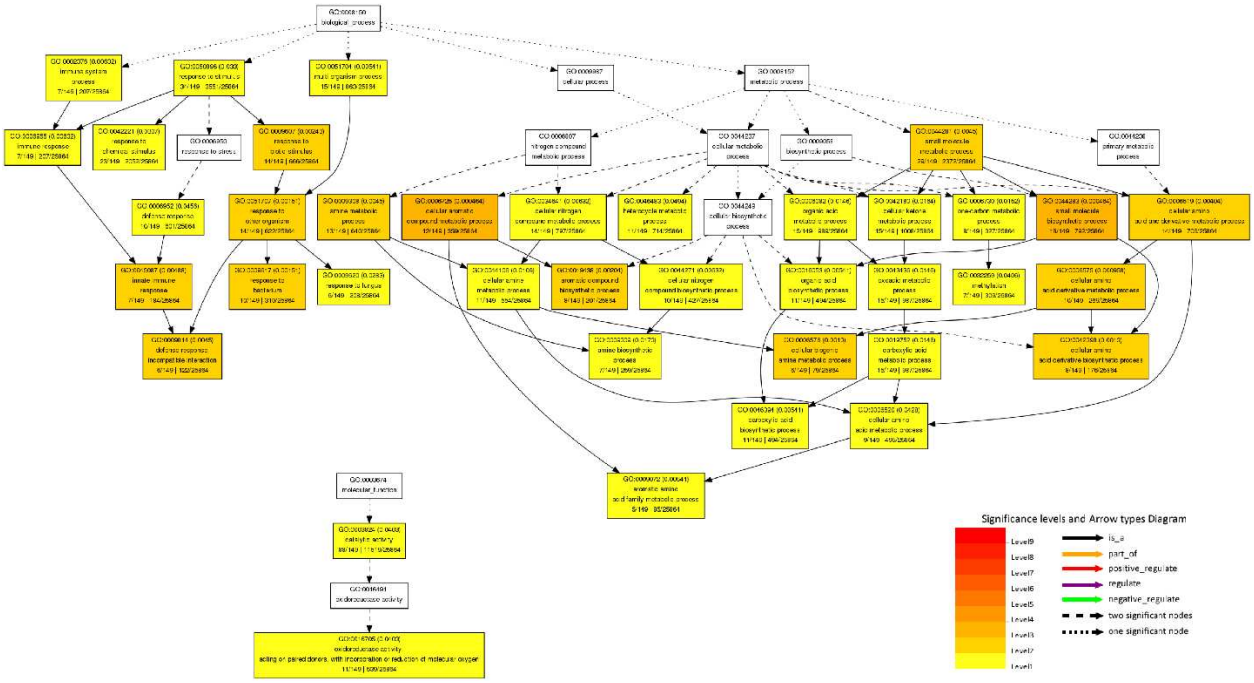

Fig. S7 Expression levels of *ZmWAK-RLK1* and BXD synthesis genes in w22 and w22Htn1

Fig. S7 Expression levels of *ZmWAK-RLK1* and BXD synthesis genes in w22 and w22Htn1. The expression of genes (A) *ZmWAK-RLK1*, (B) *Bx1*, (C) *Igl*, (D) *Bx2*, (E) *Bx3*, (F) *Bx4*, (G) *Bx5*, (H) *Bx6*, (I) *Bx7*, (J) *Bx8*, (K) *Bx9*, (L) *Bx10/11*, (M) *Bx12*, (N) *Bx13*, (O) *Glu1* and (P) *Glu2* is shown. The colors indicate time points before and after infection. The statistical analysis was conducted using Tukey's HSD in four biological replicates ($p = 0.05$). The lowercase letters represented the significant difference ($p = 0.05$). Error bars are ± SE.

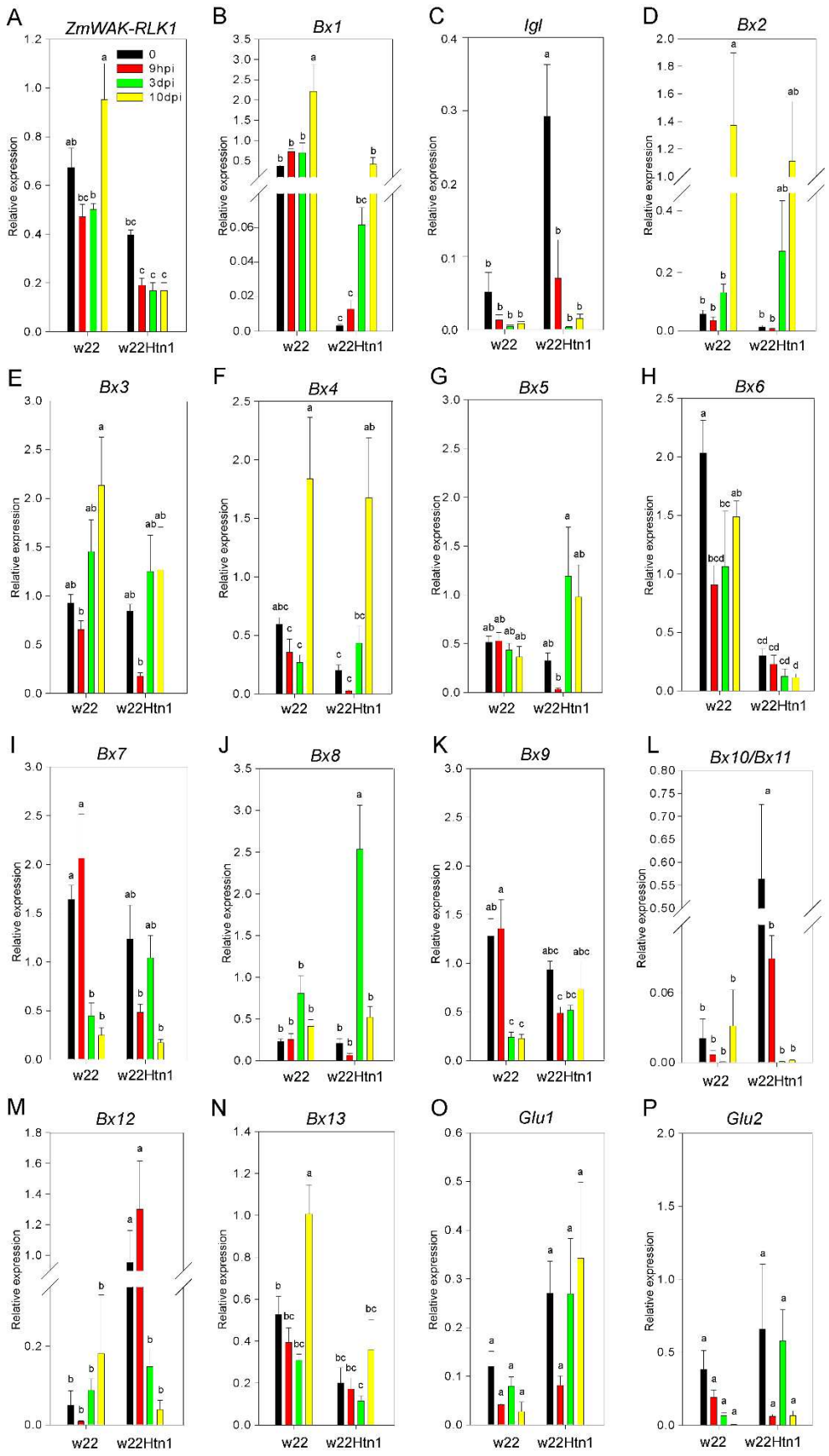
A
ZmWAK-RLK1
0
9hpi
3dpi
10dpi
B
Bx1
C
Igl
D
Bx2
E
Bx3
F
Bx4
G
Bx5
H
Bx6
I
Bx7
J
Bx8
K
Bx9
L
Bx10/Bx11
M
Bx12
N
Bx13
O
Glu1
P
Glu2
Relative expression
w22
w22Htn1

Fig. S8 Infection of *S. littoralis* and *D. balteata* in w22 and w22Htn1

Fig. S8 Infection of *S. littoralis* and *D. balteata* in w22 and w22Htn1. (A) Performance of *S. littoralis*, (B) performance of *D. balteata*, (C) leaf biomass after *S. littoralis* inoculation, (D) leaf biomass after *D. balteata* inoculation, (E) root biomass after *S. littoralis* inoculation, (F) root biomass after *D. balteata* inoculation. The statistical analysis was conducted using Sigma Plot 13 ($p = 0.05$). Error bars are ± SE.

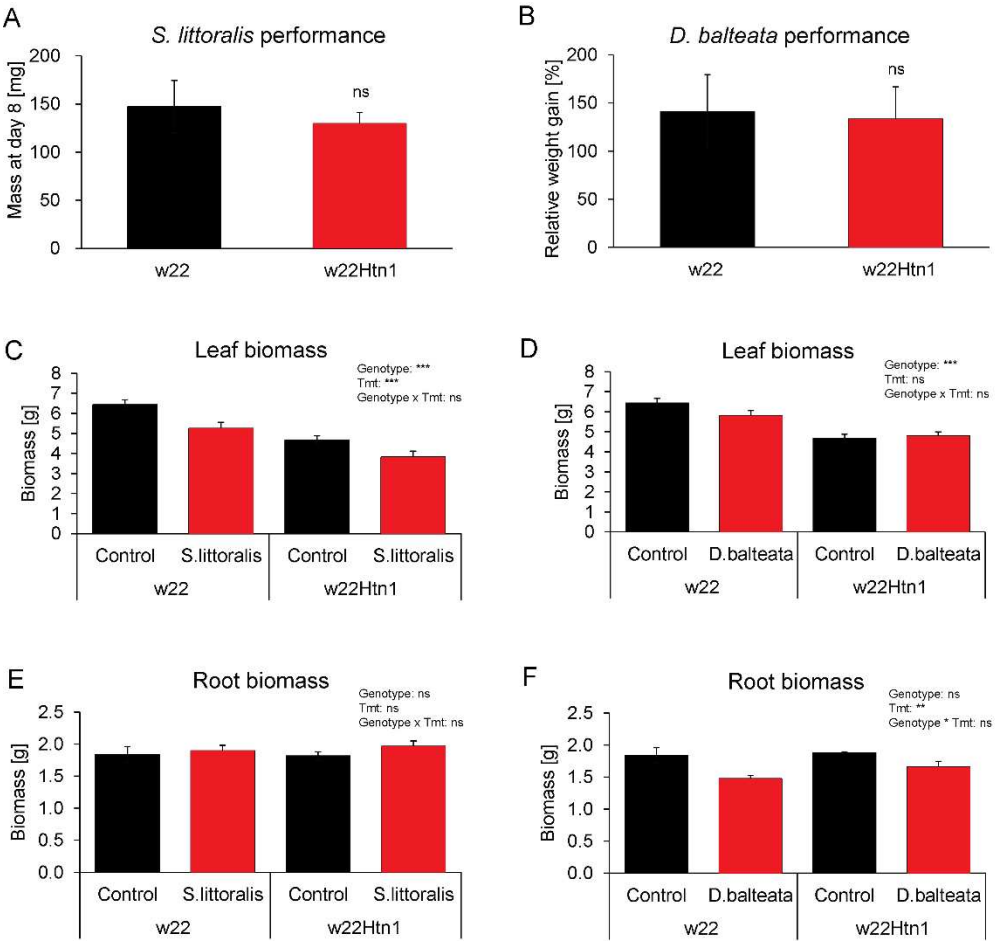

Fig. S9 Content of BXD compounds in the second leaves of bx mutants at 10 dpi

Fig. S9 Content of BXD compounds in the second leaves of bx mutants at 10 dpi. The contents of DIMBOA-Glc (A), DIMBOA (B), HMBOA-Glc (C), DIM_2BOA-Glc (D) and HDMBOA-Glc (E) were detected. HDM_2BOA-Glc is below the detection limit and not shown. w22-wt is provided by Prof. Georg Jander and represented the parental material for obtaining the bx mutants. The statistical analysis was conducted using Tukey's HSD in eight biological replicates

(p = 0.05). The lowercase letters represented the significant difference (p = 0.05). ns: no significance. Error bars are ± SE.

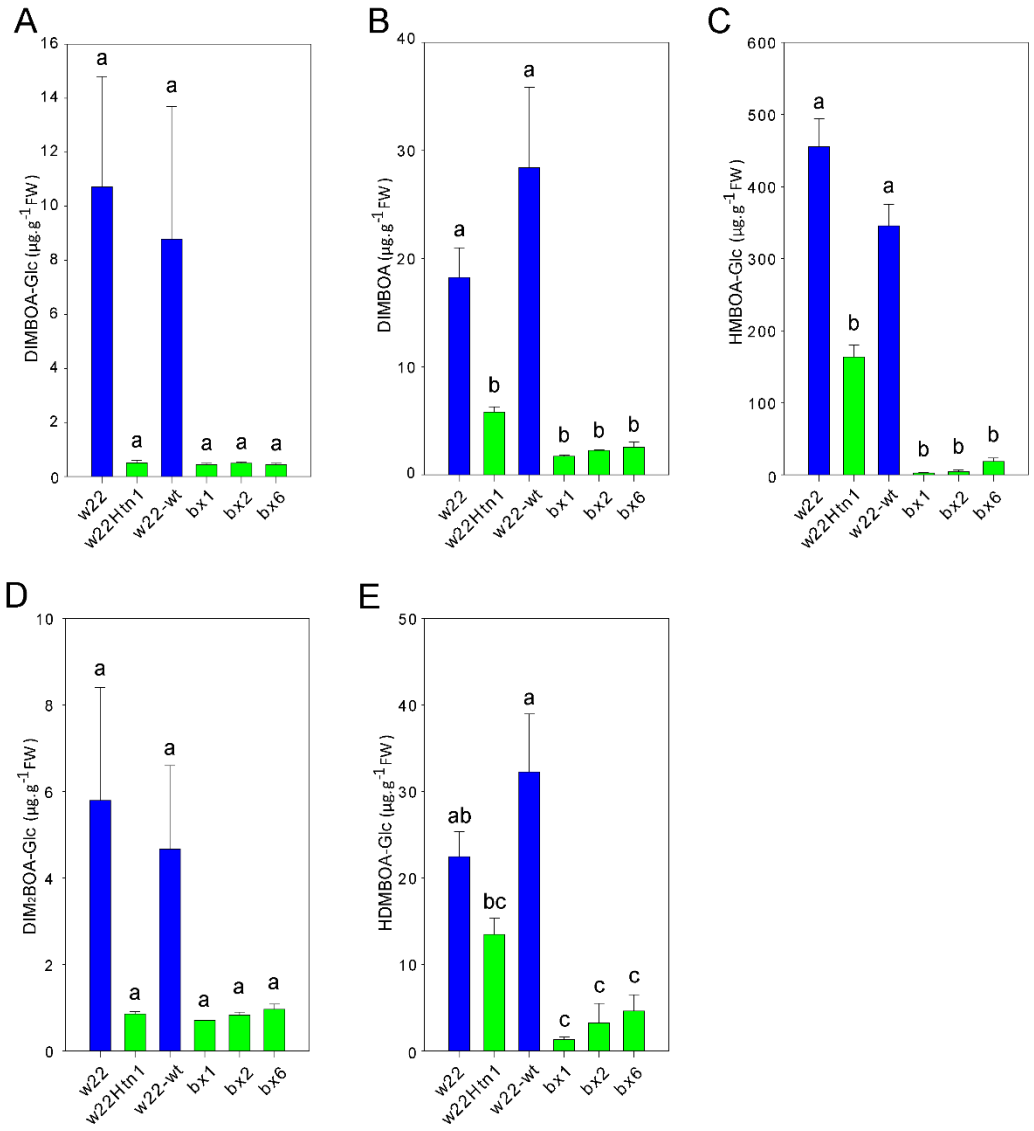

Fig. S10 Content of BXD compounds in the second leaves of *Htn1* NILs and mutants at 21 days after sowing

Fig. S10 Content of BXD compounds in the second leaves of *Htn1* NILs and mutants at 21 days after sowing. The contents of DIMBOA-Glc (A), DIMBOA (B), HMBOA-Glc (C) and HDMBOA-Glc (D) were detected. HDM_2BOA-Glc is below than the detection limit and not shown. The statistical analysis was conducted using Tukey's HSD in eight biological replicates

(p = 0.05). The lowercase letters represented the significant difference (p = 0.05). The ns stands for no significance. Error bars are ± SE.

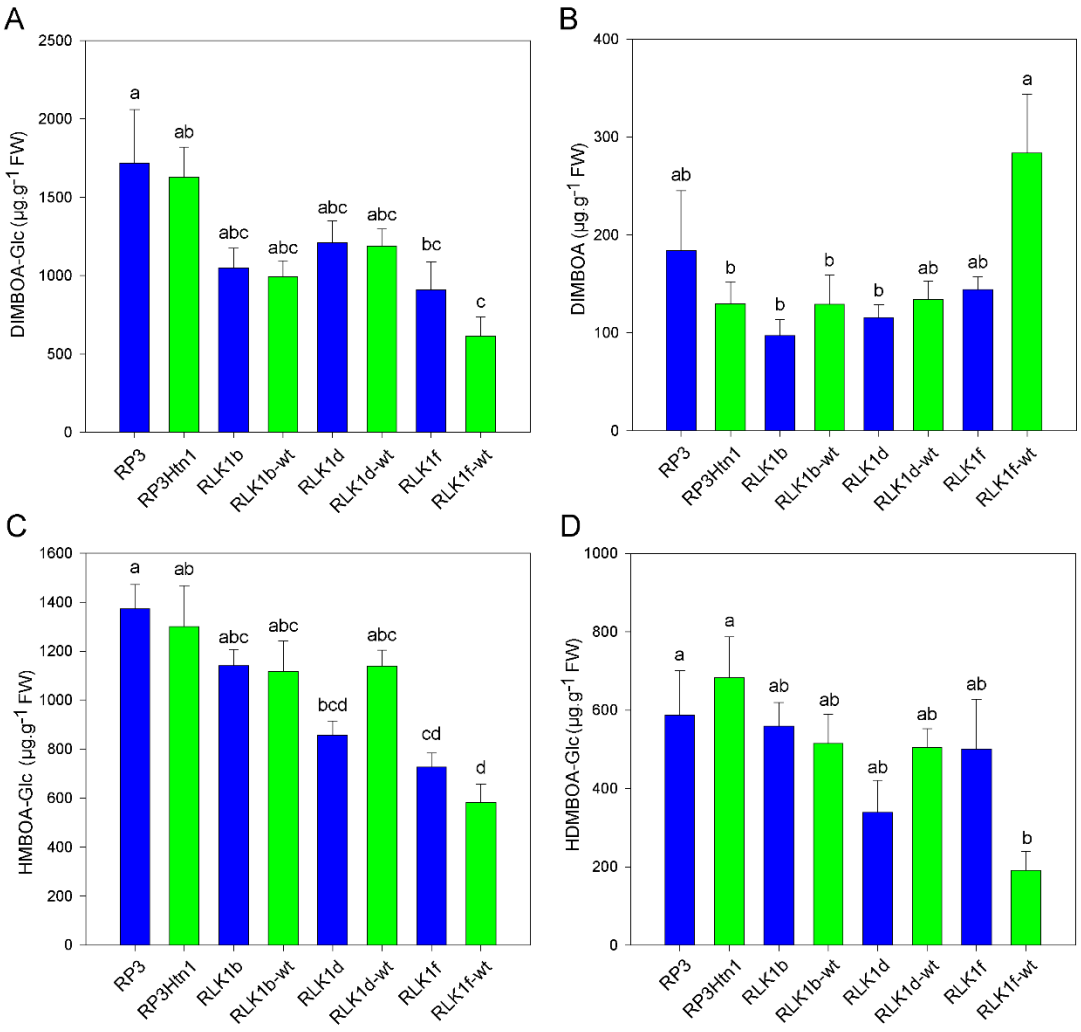

Fig. S11 Expression levels of *ZmWAK-RLK1* and BXD synthesis genes in the second leaves of *Htn1* NILs and mutants at 21 days after sowing

Fig. S11 Expression levels of *ZmWAK-RLK1* and BXD synthesis genes in the second leaves of *Htn1* NILs and mutants at 21 days after sowing. The relative transcriptional levels of *ZmWAK-RLK1* (A), *Bx1* (B), *Bx6* (C), *Bx7* (D) and *Bx13* (E) were determined(n=5). The statistical analysis was conducted using Tukey's HSD (p = 0.05) in eight biological replicates. The lowercase letters represented the significant difference (p = 0.05). ns: no significance. Error bars are ± SE.

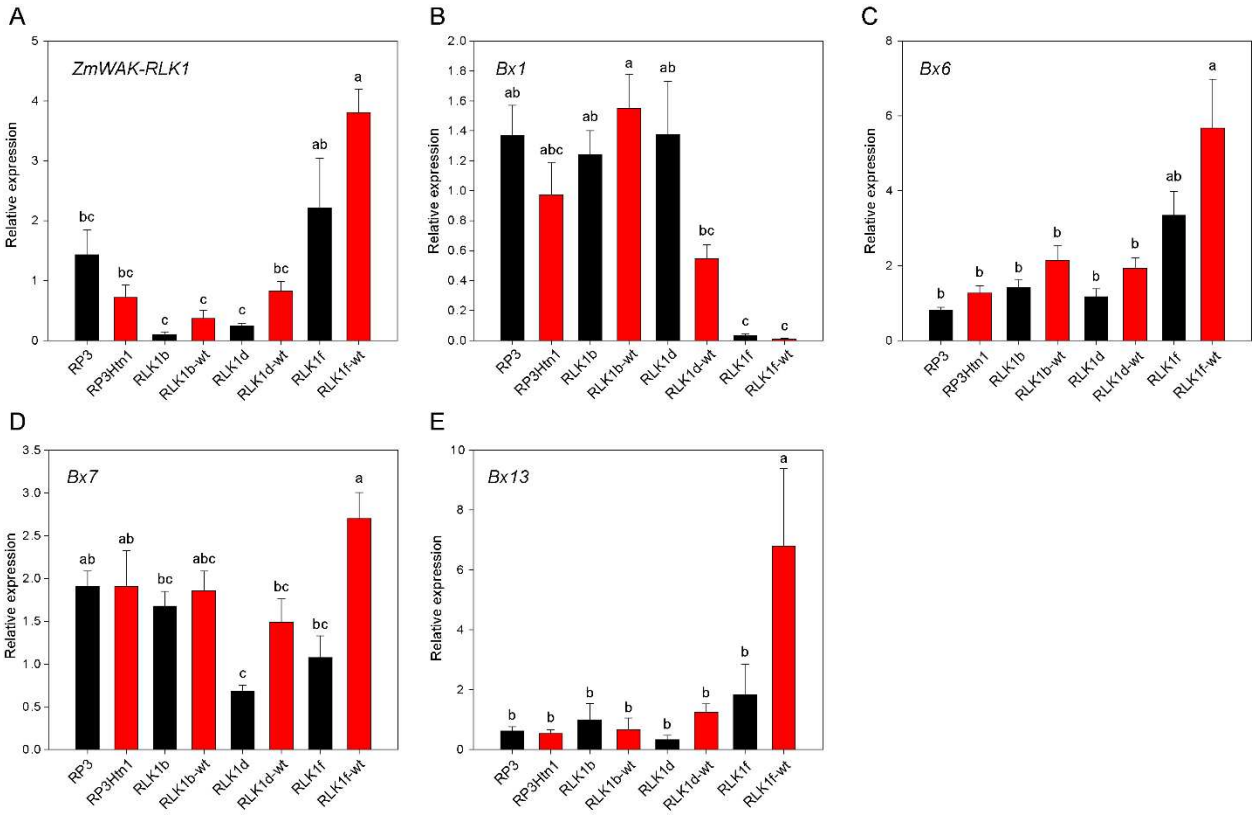

Table S1 Information of the maize genotypes with and without *Htn1* used in different experiments of this study

Table S1 Information of the maize genotypes with and without *Htn1* used in different experiments of this study

Genotypes	Genetic background	Alleles of *ZmWAK-RLK1*	Mycelium development	RNA-seq	RT-qPCR	BXD assay	Comment
w22	w22	S		Yes	Yes	Yes	Inbred line w22[a]
w22Htn1	w22	R, *Htn1*		Yes	Yes	Yes	w22 + *Htn1* introgression[a]
B37	B37	S	Yes	Yes			Inbred line B37[a]
B37Htn1	B37	R, *Htn1*	Yes	Yes			B37 + *Htn1* introgression[a]
RP3	RP3	S	Yes		Yes	Yes	Inbred line RP3[b]
RP3Htn1	RP3	R, *Htn1*	Yes		Yes	Yes	RP3 + *Htn1* introgression[b]
RLK1b	RP3Htn1	S	Yes		Yes	Yes	EMS mutant, 1365', G to A; Met to Ile[b]
RLK1b-wt	RP3Htn1	R, *Htn1*	Yes		Yes	Yes	RLK1b sister line, functional *Htn1*[b]
RLK1d	RP3Htn1	S	Yes		Yes	Yes	EMS mutant, 1490', C to T; Leu to Phe[b]
RLK1d-wt	RP3Htn1	R, *Htn1*	Yes		Yes	Yes	RLK1d sister line, functional *Htn1*[b]
RLK1f	RP3Htn1	S	Yes		Yes	Yes	EMS mutant, 1642', G to A; Gly to Arg[b]
RLK1f-wt	RP3Htn1	R, *Htn1*	Yes		Yes	Yes	RLK1f sister line, functional *Htn1*[b]

R = resistance allele *Htn1*, S = susceptible allele *htn1*. [a] and [b] are the references of Raymundo *et al.*, 1981 and Hurni *et al.*, 2015, respectively.

Table S2 Setup of RT-qPCR assays for target genes

Table S2 Setup of RT-qPCR assays for target genes

Order	Target genes	Primers (5' to 3')	PCR efficiency (E) R^2 of Calibration curve slope	Description	References
1	*Actin*	F - TACCATGTTCCCTAGGGATTG R - GTGGCGCAATCACTTTAACC	E=109.8%, R^2=0.995, Slope=-3.107	Reference gene	Bamler et al. 2013
2	*FPGS*	F - ATCTCGTTGGGGATGTCTTG R - AGCACCGTTCAAATGTCTCC	E=104.9%, R^2=0.990, Slope=-3.209	Reference gene	Hurni et al. 2015
3	*WAK-RLK1.1*	F - TATTGTTGGTGCTGTTGCCG R - GGACTCAATCCTTGTCCCTG	E=104.0%, R^2=0.996, Slope=-3.229	*WAK-RLK1*	Hurni et al. 2015
4	*BX1*	F - CCCGAGCACGTAAAGCAGAT R - CTTCATGCCCCTGGCATACT	E=100.1%, R^2=0.994, Slope=-3.319	Benzoxazinoid pathway	Ahmad et al. 2011
5	*BX2*	F - GACGAGGACGACGATAAGGACTT R - GGCCATACTCCTTCTGAAGAGACAG	E=126.1%, R^2=0.989, Slope=-2.821	Benzoxazinoid pathway	Ahmad et al. 2011
6	*BX3*	F - ATGGCCGAGCTCATCAACAA R - TCGTCCTCACCTCCGTCTGT	E=107.4%, R^2=0.994, Slope=-3.156	Benzoxazinoid pathway	Ahmad et al. 2011
7	*BX4*	F - TGTTCCTCCGGATCATCTGC R - AAGAGGCTGTCCCACCGCT	E=100.9%, R^2=0.994, Slope=-3.300	Benzoxazinoid pathway	Ahmad et al. 2011
8	*Bx5*	F - CCATTTCGACTGGGAGGTCC R - GTCCATGCTCACCTTCCAGC	E=109.7%, R^2=0.992, Slope=-3.109	Benzoxazinoid pathway	Ahmad et al. 2011
9	*BX6*	F - AAGTTCAACACCATAGGACTCGATG R - CAGGTAGCTAGAGCCTGAAGTGGTC	E=107.6%, R^2=0.961, Slope=-3.153	Benzoxazinoid pathway	Ahmad et al. 2011
10	*BX7*	F - GGCTGGGTTCCGTGACTACA R - GACCTCGATGATGGACGGG	E=106.9%, R^2=0.989, Slope=-3.167	Benzoxazinoid pathway	Ahmad et al. 2011
11	*BX8*	F - GGAAGAGGATGAACGAGCTCAA R - GACCCAGCAGATTCATCGATG	E=114.0%, R^2=0.987, Slope=-3.027	Benzoxazinoid pathway	Ahmad et al. 2011
12	*BX9*	F - GGGACCAGTTCGGCAACAT R - TGCCCACCTTCCACACGT	E=117.3%, R^2=0.999, Slope=-2.967	Benzoxazinoid pathway	Ahmad et al. 2011
13	*BX10 + BX11*	F - CAGCAGGTGGTGGTGATAAT R - AGCGCCAGACTCACAAAGG	E=109.5%, R^2=0.999, Slope=-3.114	Benzoxazinoid pathway	Meilhs et al. 2013
14	*BX12*	F - GCCCACCCAAGTAAGCTTCG R - AGAGACAGCGATAGGATGGA	E=95.4%, R^2=0.996, Slope=-3.437	Benzoxazinoid pathway	Meilhs et al. 2013
15	*BX13*	F - CATCGTGTGCCAGTACTACC R - ACCGGTCATTCGTCACAAGC	E=99.3%, R^2=0.961, Slope=-3.340	Benzoxazinoid pathway	Handrick et al. 2016
16	*IGL*	F - GCCTCATAGTTCCCGACCTC R - GAATCCTCGTGAAGCTCGTG	E=111.8%, R^2=0.996, Slope=-3.069	Benzoxazinoid pathway	Ahmad et al. 2011
17	*GLU1*	F - CCTCATGATGTGGGTGCAG R - ATGCATGACAAGGCCAGACT	E=110.6%, R^2=0.998, Slope=-3.092	Benzoxazinoid pathway	Ahmad et al. 2011
18	*GLU2*	F - AAAAACATGGGACCTCGTGA R - ATTGCATGACGACAATGCTAGA	E=110.4%, R^2=0.985, Slope=-3.095	Benzoxazinoid pathway	Ahmad et al. 2011

Note: The expression of gene *Bx14* was analyzed by using the published primers (Handrick et al. 2016). However, this primer combination didn't work in experiments.

Table S3 Statistics of RNA-seq reads sequenced and mapped

Table S3 Statistics of RNA-seq reads sequenced and mapped

Sample number	Samples	Raw reads	Uniquely mapped reads[a]	Percentage of uniquely mapped reads (%)	Percentage of multi-mapped reads (%)	Percentage of unmapped reads (%)
1	0-w22-1	19,894,158	12,757,882	64.13	12.66	20.34
2	0-w22-2	25,718,662	18,612,570	72.37	6.63	20.18
3	0-w22-3	24,937,383	17,948,211	71.97	6.41	20.85
4	0-w22Htn1-1	27,452,042	20,264,307	73.82	5.96	19.70
5	0-w22Htn1-2	19,815,200	14,439,891	72.87	6.07	20.44
6	0-w22Htn1-3	24,173,527	16,215,534	67.08	9.55	21.40
7	0-B37-1	22,180,888	14,689,311	66.23	5.27	28.03
8	0-B37-2	24,474,895	18,273,286	74.66	5.96	18.75
9	0-B37-3	27,774,311	20,221,020	72.80	6.73	19.74
10	0-B37Htn1-1	26,728,646	19,277,404	72.12	6.16	21.04
11	0-B37Htn1-2	24,336,731	17,640,859	72.49	6.06	20.82
12	0-B37Htn1-3	22,625,055	16,499,617	72.93	6.15	20.30
13	9h-w22-1	25,343,283	17,460,901	68.90	7.81	22.49

14	9h-w22-2	26,384,078	18,489,206	70.08	7.16	22.03
15	9h-w22-3	21,846,924	13,680,343	62.62	5.97	30.81
16	9h-w22Htn1-1	34,074,874	23,121,230	67.85	6.27	25.40
17	9h-w22Htn1-2	24,276,403	17,299,847	71.26	7.02	21.07
18	9h-w22Htn1-3	30,200,422	20,381,456	67.49	7.23	24.62
19	9h-B37-1	17,962,777	12,878,288	71.69	7.38	20.10
20	9h-B37-2	23,815,810	16,892,476	70.93	7.12	21.22
21	9h-B37-3	24,188,988	17,604,433	72.78	7.15	19.38
22	9h-B37Htn1-1	25,195,971	17,304,100	68.68	7.80	22.65
23	9h-B37Htn1-2	23,902,398	16,173,755	67.67	7.27	24.40
24	9h-B37Htn1-3	24,731,481	17,279,056	69.87	7.13	22.39
25	3d-w22-1	22,399,000	15,772,632	70.42	6.44	22.49
26	3d-w22-2	26,175,191	18,816,409	71.89	6.43	21.06
27	3d-w22-3	23,253,678	16,758,123	72.07	6.45	20.82
28	3d-w22Htn1-1	23,878,639	17,185,076	71.97	5.92	21.58
29	3d-w22Htn1-2	20,568,384	14,338,420	69.71	7.09	22.35
30	3d-w22Htn1-3	34,008,596	24,127,141	70.94	5.81	22.76
31	3d-B37-1	23,690,913	14,726,042	62.16	4.70	32.71
32	3d-B37-2	27,646,350	19,934,380	72.10	5.89	21.42
33	3d-B37-3	21,114,803	16,208,484	76.76	5.69	16.98
34	3d-B37Htn1-1	21,758,134	15,409,264	70.82	5.68	23.03
35	3d-B37Htn1-2	27,236,811	19,866,766	72.94	5.84	20.68
36	3d-B37Htn1-3	22,700,637	16,553,064	72.92	5.60	21.00
37	10d-w22-1	23,051,842	16,566,330	71.87	6.16	21.24
38	10d-w22-2	28,611,557	20,463,896	71.52	6.01	21.77
39	10d-w22-3	12,829,435	7,480,564	58.31	4.82	36.38
40	10d-w22Htn1-1	24,435,356	17,199,294	70.39	5.45	23.76
41	10d-w22Htn1-2	28,996,022	21,442,119	73.95	5.78	19.69
42	10d-w22Htn1-3	18,649,090	13,429,238	72.01	5.78	21.71
43	10d-B37-1	13,275,463	9,658,508	72.75	5.46	21.16
44	10d-B37-2	15,217,491	11,288,257	74.18	5.38	19.89
45	10d-B37-3	23,349,541	17,096,788	73.22	5.36	20.83
46	10d-B37Htn1-1	20,104,137	14,270,397	70.98	4.94	23.79
47	10d-B37Htn1-2	38,203,107	27,216,898	71.24	5.40	22.82
48	10d-B37Htn1-3	26,094,601	18,820,165	72.12	5.61	21.68
	Total	1,159,283,685	820,033,238	70.74	NA[b]	NA[b]
	Mean	24,151,743	17,084,026	70.74	NA[b]	NA[b]

[a] Parameters for mapping: less than 1% mismatch, 1 locus mapped, intron size is less than 10 kb.
[b] NA = not analyzed.

References

Ahmad S, Veyrat N, Gordon-Weeks R, Zhang YH, Martin J, Smart L, Glauser G, Erb M, Flors V, Frey M, Ton J. 2011. Benzoxazinoid metabolites regulate innate immunity against aphids and fungi in maize. *Plant Physiology* **157**(1): 317-327.

Balmer D, de Papajewski DV, Planchamp C, Glauser G, Mauch-Mani B. 2013. Induced resistance in maize is based on organ-specific defence responses. *Plant Journal* **74**(2): 213-225.

Du Z, Zhou X, Ling Y, Zhang ZH, Su Z. 2010. agriGO: a GO analysis toolkit for the agricultural community. *Nucleic Acids Research* **38**: W64-W70.

Handrick V, Robert CAM, Ahern KR, Zhou SQ, Machado RAR, Maag D, Glauser G, Fernandez-Penny FE, Chandran JN, Rodgers-Melnik E, Schneider B, Buckler ES, Boland W, Gershenzon J, Jander G, Erb M, Kollner TG. 2016. Biosynthesis of 8-o-methylated benzoxazinoid defense compounds in maize. *Plant Cell* **28**(7): 1682-1700.

Hurni S, Scheuermann D, Krattinger SG, Kessel B, Wicker T, Herren G, Fitze MN, Breen J, Presterl T, Ouzunova M, Keller B. 2015. The maize disease resistance gene *Htn1* against northern corn leaf

blight encodes a wall-associated receptor-like kinase. *Proceedings of the National Academy of Sciences of the United States of America* **112**(28): 8780-8785.

Meihls LN, Handrick V, Glauser G, Barbier H, Kaur H, Haribal MM, Lipka AE, Gershenzon J, Buckler ES, Erb M, Kollner TG, Jander G. 2013. Natural variation in maize aphid resistance is associated with 2,4-dihydroxy-7-methoxy-1,4-benzoxazin-3-one glucoside methyltransferase activity. *Plant Cell* **25**(6): 2341-2355.

Raymundo AD, Hooker AL, Perkins JM. 1981. Effect of gene *HtN* on the development of northern corn leaf blight epidemics. *Plant Disease* **65**(4): 327-330.

Robinson MD, McCarthy DJ, Smyth GK. 2010. edgeR: a Bioconductor package for differential expression analysis of digital gene expression data. *Bioinformatics* **26**(1): 139-140.

Table S4 The logFC and annotation of 215 differently expressed genes

		0		9 hpi		3 dpi		10 dpi				
Number	DEGs	w22Htn1 vs. w22	B37Htn1 vs. B37	w22Htn1 vs. w22	B37Htn1 vs. B37	w22Htn1 vs. w22	B37Htn1 vs. B37	w22Htn1 vs. w22	B37Htn1 vs. B37	Annotation	Best hit in rice	Category
1	GRMZM2G085661			-6.35	-5.03					bx2 - benzoxazinone synthesis 2	n.a	Benzoxazinoids pathway
2	GRMZM2G015892			3.96	4.52					Indole-3-glycerol phosphate lyase chloroplast precursor	LOC_Os03g58300.1	Benzoxazinoids pathway
3	GRMZM6G617209					-2.06	-2.13			BX6 - Benzoxazinone synthesis 6	LOC_Os03g48430.1	Benzoxazinoids pathway
4	GRMZM2G336824	11.02	4.32							BX11 - Benzoxazinone synthesis 11	LOC_Os12g25870.1	Benzoxazinoids pathway
5	GRMZM2G127418	6.93	5.84							BX14 - Benzoxazinone Synthesis 14	LOC_Os05g43940.1	Benzoxazinoids pathway
6	GRMZM2G000236			4.37	4.57					OPR2 - 12-oxo-phytodienoic acid reductase2	LOC_Os06g11290.1	JAs pathway
7	GRMZM2G109130	4.41	4.28							LOX3 - Lipoxygenase 3	LOC_Os03g49350.1	JAs pathway
8	GRMZM2G077316			-4.95	-2.51			-4.44	-3.91	AOC1 - Allene oxide cyclase 1	LOC_Os03g32314.1	JAs pathway
9	GRMZM2G166616	4.90	4.45							ACCO3 - 1-aminocyclopropane-1-carboxylate oxidase 3	LOC_Os05g05680.1	Ethylene pathways
10	GRMZM2G332423	6.46	3.88							ACCO4 - 1-aminocyclopropane-1-carboxylate oxidase 4	LOC_Os05g05680.1	Ethylene pathways
11	GRMZM2G054123	3.90	2.38							S-adenosylmethionine synthase	LOC_Os01g22010.1	Lignin pathway
12	GRMZM2G099363	2.72	3.19							OMT2 - Caffeoyl-CoA O-methyltransferase 2	LOC_Os06g06980.1	Lignin pathway
13	GRMZM2G127948	2.53	3.02							OMT1 - Caffeoyl-CoA O-methyltransferase 1	LOC_Os06g06980.1	Lignin pathway
14	AC209784.3_FG007			2.06	2.65					*DnaK family protein putative expressed	LOC_Os05g38530.1	Defense
15	GRMZM2G032856	2.68	2.11							Glutathione S-transferase GST 24	LOC_Os01g72150.1	Defense
16	GRMZM2G042639	6.65	6.69	3.03	4.75	2.71	3.78			SAF1 - Safener induced 1; Glutathione S-transferase	LOC_Os03g17480.1	Defense
17	GRMZM2G044383					3.47	2.55			Glutathione S-transferase GST 30	LOC_Os10g38740.1	Defense
18	GRMZM2G065585	3.32	4.23							GEB1 - Glucan endo-1,3-beta-glucosidase homolog 1	LOC_Os01g71340.1	Defense
19	GRMZM2G074743	5.92	5.39							AOX3 - Alternative Oxidase 3	LOC_Os04g57320.1	Defense
20	GRMZM2G145461	3.48	3.04			2.52	3.10			CHN2 - Chitinase 2	LOC_Os03g30470.1	Defense
21	GRMZM2G156632	3.91	3.79							WIP1 - wound induced protein1	LOC_Os01g04050.1	Defense
22	GRMZM2G162505	2.03	2.33							*Chitinase 2 putative expressed	LOC_Os10g28050.1	Defense
23	GRMZM2G150762			-5.63	-2.95					HIR2 - hypersensitive induced response 2	LOC_Os09g19710.1	Defense
24	GRMZM2G157869	-5.70	-3.88	#####	-9.71	-5.17	-3.41	-5.43	-6.05	*Hypersensitive-induced response protein putative expressed	LOC_Os09g19710.1	Defense
25	GRMZM2G063392	6.33	12.71							TKL_IRAK_DUF26-la.6 - DUF26 kinases	LOC_Os10g04730.1	Receptor like kinase
26	GRMZM2G303909	2.15	4.45							*Receptor-like protein kinase, putative expressed	LOC_Os04g12600.1	Receptor like kinase
27	GRMZM2G433684	4.68	12.64	5.67	13.12	5.00	11.08	3.80	11.24	*LRR receptor kinase putative expressed	LOC_Os02g40240.1	Receptor like kinase
28	GRMZM2G438871	2.70	3.94							*Lectin-like receptor kinase putative expressed	LOC_Os07g18240.1	Receptor like kinase
29	GRMZM2G466298	2.46	3.23							*Lectin-like protein kinase putative expressed	LOC_Os02g48210.1	Receptor like kinase
30	GRMZM2G009770	-5.50	-6.84							*receptor-like protein kinase precursor putative expressed	LOC_Os02g12400.1	Receptor like kinase
31	GRMZM2G165387	-6.70	-3.46	-7.67	-3.20	-5.95	-2.59	-5.12	-2.61	*Receptor-like protein kinase 5 precursor	LOC_Os02g40180.1	Receptor like kinase
32	GRMZM2G436455	-6.82	-8.20	-4.40	-9.40	-2.71	-9.96	-2.76	#####	*Resistance-related receptor-like kinase putative expressed	LOC_Os01g02810.1	Receptor like kinase
33	GRMZM2G089836	3.28	3.40			2.98	5.03			Beta-fructofuranosidase 1; IVR2 - invertase 2	LOC_Os02g01590.1	Cell wall
34	GRMZM2G123107	3.17	4.69							Glycosyl hydrolases family 17 putative expressed	LOC_Os01g71410.1	Cell wall
35	GRMZM2G125032	2.89	5.88							Beta-1,3-glucanase	LOC_Os01g71670.1	Cell wall
36	GRMZM2G162359	4.34	2.46							*Glycosyl hydrolase putative expressed	LOC_Os06g25010.1	Cell wall
37	GRMZM2G135966	-2.72	#####	-3.90	-8.50	-5.99	#####			*Glycosyl hydrolase family 47 domain contain protein expressed	LOC_Os04g51690.1	Cell wall
38	AC214360.3_FG001			3.58	3.10					KS4 - Kaurene Synthase 4	LOC_Os02g36220.1	Secondary metabolism
39	GRMZM2G067225	2.06	3.84							Putative cytochrome P450 superfamily protein	LOC_Os03g12500.1	Secondary metabolism
40	GRMZM2G070304	8.75	5.70							Glycerol-3-phosphate acyltransferase putative expressed	LOC_Os11g45400.1	Secondary metabolism
41	GRMZM2G087875	2.96	3.84							Putative cytochrome P450 superfamily protein	LOC_Os03g55240.1	Secondary metabolism
42	GRMZM2G106950	3.11	3.13							Indole-3-glycerol phosphate synthase chloroplast precursor	LOC_Os09g08130.2	Secondary metabolism
43	GRMZM2G117878	3.35	4.60							*Cytokinin-N-glucosyltransferase putative expressed	LOC_Os07g13800.1	Secondary metabolism
44	GRMZM2G140817	3.13	2.92							Amino acid permease	LOC_Os04g35540.1	Secondary metabolism
45	GRMZM2G145242	2.36	2.79							Putative cytochrome P450 superfamily protein	LOC_Os05g41440.1	Secondary metabolism
46	GRMZM2G146206					-2.46	-2.81	-2.37	-5.28	TPI5 - triose phosphate isomerase 5	LOC_Os01g62420.4	Secondary metabolism
47	GRMZM2G132550	4.15	4.52							bHLH124 - bHLH-transcription factor 124	LOC_Os01g09990.1	Transcription factors
48	GRMZM2G395749	3.30	2.79							Putative MYB DNA-binding domain superfamily protein	LOC_Os01g09760.1	Transcription factors
49	GRMZM2G421256	2.11	2.03							MYB20 - MYB-related-transcription factor 20	LOC_Os04g49450.1	Transcription factors
50	GRMZM2G425430			5.64	4.38	6.06	3.86	4.81	4.84	*WRKY81	LOC_Os03g33012.1	Transcription factors
51	AC193786.3_FG005			-3.92	-3.17					bHLH54 - bHLH-transcription factor 54	LOC_Os01g72370.1	Transcription factors
52	GRMZM2G305901	-6.40	#####							Zinc finger C3HC4 type domain containing protein expressed	LOC_Os01g06590.1	Transcription factors
53	GRMZM2G326783	2.24	2.74	3.30	2.22	2.49	2.52	2.33	3.45	THXTrihelix-transcription factor 29	LOC_Os02g33610.1	Transcription factors
54	GRMZM2G016150	-4.86	-3.06							OHP1 - Opaque2 Heterodimerizing Protein1	LOC_Os03g58250.1	
55	AC196502.3_FG003	8.65	4.81							*Proline-rich family protein putative expressed	LOC_Os07g44830.1	
56	AC206788.3_FG015	2.19	2.23							*Anthocyanidin 5 3-O-glucosyltransferase putative expressed	LOC_Os05g45100.1	
57	GRMZM2G002173	3.25	5.27	2.88	3.96	2.88	2.82	5.22	3.31	Phosphopantothenate cysteine ligase	LOC_Os02g36550.1	
58	GRMZM2G004349	3.10	2.15							Seed maturation protein	LOC_Os05g45050.2	
59	GRMZM2G006219	3.38	2.54			3.82	2.88			*Major sperm protein (MSP) domain containing protein	LOC_Os02g42940.1	
60	GRMZM2G006878	4.86	3.69	5.70	4.37	5.86	2.78			Expressed protein	LOC_Os03g63870.1	
61	GRMZM2G009045	5.11	3.95	3.04	5.89					Phosphate transporter 3;2	LOC_Os09g28160.1	
62	GRMZM2G010048	5.55	2.92							Thaumatin family domain containing protein expressed	LOC_Os03g46060.1	
63	GRMZM2G010596	2.97	2.20							3-methyl-2-oxobutanoate hydroxymethyltransferase	LOC_Os01g12560.1	
64	GRMZM2G011253	3.33	2.10							60S ribosomal protein L31	LOC_Os08g39500.1	
65	GRMZM2G011523	3.41	4.92							BBTI11 - Bowman-Birk type bran trypsin inhibitor precursor putative expressed	LOC_Os01g04040.1	
66	GRMZM2G011559	2.13	2.39							Alpha-soluble NSF attachment protein	LOC_Os08g18110.1	
67	GRMZM2G020471					2.40	8.94	2.19	9.24	Uncharacterized protein	n.a	
68	GRMZM2G022972	2.45	5.15							Calmodulin binding protein putative expressed	LOC_Os01g04280.1	
69	GRMZM2G031177	2.50	2.18							*MATE efflux family protein putative expressed	LOC_Os03g08900.1	
70	GRMZM2G032910	2.24	2.29							*Hydrolase alpha/beta fold family domain containing protein expressed	LOC_Os10g35520.1	
71	GRMZM2G033226	2.36	2.60							*ATP-citrate synthase subunit 1 putative expressed	LOC_Os01g19450.1	
72	GRMZM2G039445	2.02	2.38			2.50	2.69	2.97	2.66	Uncharacterized protein	LOC_Os02g42730.1	
73	GRMZM2G039639	3.11	2.71							Protein P21	LOC_Os03g46070.1	
74	GRMZM2G043191	3.57	2.19							Inositol polyphosphate 5-phosphatase 11	LOC_Os03g42810.2	
75	GRMZM2G044128	2.88	2.35							*h/ACA ribonucleoprotein complex subunit 4 putative expressed	LOC_Os07g44190.1	
76	GRMZM2G045534	2.26	2.56							*ATP-citrate synthase subunit 1 putative expressed	LOC_Os01g19450.1	
77	GRMZM2G047187			3.08	6.92	4.59	3.50	2.97	4.61	*Transporter major facilitator family putative expressed	LOC_Os11g05390.1	
78	GRMZM2G048287	2.14	2.35							Uncharacterized protein	LOC_Os03g10410.1	
79	GRMZM2G054522	2.92	3.59			2.90	2.25	2.85	2.25	Uncharacterized protein	LOC_Os02g46956.1	
80	GRMZM2G054900	2.26	2.86			4.09	3.23			Putative calmodulin-binding family protein	LOC_Os01g38980.2	
81	GRMZM2G056513	2.27	5.14							Expressed protein	LOC_Os04g56390.1	
82	GRMZM2G057652	5.35	2.04					2.14	6.70	*OsRhmbd8 - Putative Rhomboid homologue expressed	LOC_Os03g24390.1	
83	GRMZM2G060210	5.26	2.55							Transferase family protein putative expressed	LOC_Os05g08640.1	
84	GRMZM2G064640	2.33	2.25							Ribosomal protein S9	LOC_Os03g05980.1	
85	GRMZM2G067242	2.35	2.19							*AAA-type ATPase family protein putative expressed	LOC_Os02g46990.1	
86	GRMZM2G074462	5.22	4.37	4.83	3.90	4.77	5.90	4.70	6.15	Putative starch binding domain containing family protein	LOC_Os01g63810.1	
87	GRMZM2G074611	2.28	2.70							Dirigent protein	LOC_Os01g25030.1	
88	GRMZM2G075505	3.98	2.75							*Nucleic acid binding protein putative expressed	LOC_Os03g06980.1	
89	GRMZM2G078725			3.35	2.69					Microtubule-associated protein TORTIFOLIA1	LOC_Os02g50640.1	
90	GRMZM2G078876	2.21	3.07							Xylogen protein 1	LOC_Os03g26820.1	
91	GRMZM2G080178			5.83	3.97					*Sulfate transporter putative expressed	LOC_Os08g31410.1	
92	GRMZM2G084825			2.08	2.30	2.69	2.10			Protein kinase	LOC_Os10g04720.1	
93	GRMZM2G090245	4.78	7.33							*Cupin domain containing protein expressed	LOC_Os08g35750.1	
94	GRMZM2G099092	2.47	7.68							Beta-expansin precursor putative expressed	LOC_Os06g47360.1	
95	GRMZM2G099467	3.32	2.21							Gibberellin 20 oxidase 2	LOC_Os10g39140.1	
96	GRMZM2G099491	2.43	2.28							Systemin receptor SR160	LOC_Os03g58110.1	
97	GRMZM2G104836	2.11	3.55							Glycine-rich protein A3	LOC_Os08g28560.1	
98	GRMZM2G112456	3.02	2.39							Oligopeptide transporter 4	LOC_Os02g46860.1	
99	GRMZM2G114692	2.53	3.59							Uncharacterized protein	LOC_Os03g61560.1	
100	GRMZM2G114775	2.72	2.29							GAGA18 - C2C2-GATA-transcription factor 18	LOC_Os03g61570.2	
101	GRMZM2G115422	9.65	3.08	2.98	2.96	6.70	6.51			*Transferase family protein putative expressed	LOC_Os01g63480.1	
102	GRMZM2G117707	6.18	2.78							Phospho-2-dehydro-3-deoxyheptonate aldolase 1	LOC_Os07g42960.1	
103	GRMZM2G120475	2.64	3.48			4.61	6.91			Uncharacterized protein	n/a	
104	GRMZM2G122126	2.85	2.37							6-phosphogluconolactonase putative expressed	LOC_Os08g43370.1	
105	GRMZM2G125196	5.99	4.72							NADP-dependent oxidoreductase putative expressed	LOC_Os11g14910.1	
106	GRMZM2G127328	3.76	4.49							LHT1, A Lysine- and Histidine-Specific Amino Acid Transporter	LOC_Os08g03350.1	
107	GRMZM2G135834	2.42	3.13			2.63	2.31	2.81	5.44	DEK C terminal domain containing protein expressed	LOC_Os03g29960.1	
108	GRMZM2G136508	2.26	4.08							*DEK C terminal domain containing protein expressed	LOC_Os03g29960.1	
109	GRMZM2G148998	5.11	7.64							Uncharacterized protein	LOC_Os07g37156.1	
110	GRMZM2G149751	2.70	2.33							*Homocysteine methyltransferase putative expressed	LOC_Os12g42884.1	
111	GRMZM2G150876	2.60	4.37							*TBC domain containing protein expressed	LOC_Os02g56570.1	
112	GRMZM2G154223			3.10	3.40					Uncharacterized protein	LOC_Os04g33110.1	
113	GRMZM2G154523	8.09	9.36							Patatin putative expressed	LOC_Os11g39990.1	
114	GRMZM2G159636	6.92	10.73	9.92	10.05	10.67	11.04	7.06	10.88	*B12D protein	LOC_Os07g17310.1	
115	GRMZM2G161696	2.50	2.25			4.17	2.10			Lysosomal protective protein	LOC_Os02g42310.1	
116	GRMZM2G162697	2.41	2.15							DNA-directed RNA polymerase II 23 kDa polypeptide	LOC_Os12g04510.1	
117	GRMZM2G167875	2.20	2.35							*60S ribosomal protein L18a putative expressed	LOC_Os01g54870.1	
118	GRMZM2G168431	2.01	2.94							Aspartic proteinase nepenthesin-2 precursor putative expressed	LOC_Os01g42320.1	
119	GRMZM2G169261			2.83	4.24					Fatty acid desaturase putative expressed	LOC_Os07g23410.1	
120	GRMZM2G176301	4.95	6.94	7.66	7.28	4.93	8.04	4.06	7.28	*Fatty acid hydroxylase putative expressed	LOC_Os11g48020.1	
121	GRMZM2G176472	2.73	3.68							*Calmodulin binding protein	LOC_Os12g36110.1	
122	GRMZM2G178807	2.00	2.36							60S ribosomal protein L7 putative expressed	LOC_Os08g13690.1	
123	GRMZM2G179170	2.47	2.60							*ATP-citrate synthase subunit 1 putative expressed	LOC_Os01g19450.2	
124	GRMZM2G310795			2.12	2.35	2.09	2.44			*Glycosyltransferase family protein 1 putative expressed	LOC_Os01g43380.1	
125	GRMZM2G310947	3.08	4.84							Cell Division Protein AAA ATPase family	LOC_Os12g24320.1	
126	GRMZM2G319138			3.60	6.97					*Pleiotropic drug resistance protein putative expressed	LOC_Os11g37700.1	
127	GRMZM2G329737	9.32	10.30	9.93	10.57	6.62	10.68	9.84	10.62	*40S ribosomal protein S4 putative expressed	LOC_Os01g25610.1	
128	GRMZM2G339562			2.05	3.56					UP-9A putative expressed	LOC_Os10g36610.1	
129	GRMZM2G345700	2.16	5.99							36.4 kDa proline-rich protein	LOC_Os04g52250.1	
130	GRMZM2G354909	3.58	2.02							Short-chain dehydrogenase/reductase putative expressed	LOC_Os04g44980.1	
131	GRMZM2G365160	6.24	2.68							*Phospho-2-dehydro-3-deoxyheptonate aldolase chloroplast precursor	LOC_Os07g42960.1	
132	GRMZM2G368591	9.75	10.26	8.24	8.67	9.83	10.57	10.09	8.26	*Integral membrane protein DUF6 containing protein expressed	LOC_Os12g33300.1	
133	GRMZM2G373522			3.00	2.41					Dehydrin; Uncharacterized protein	LOC_Os02g44870.1	
134	GRMZM2G387227	5.55	7.50	5.64	7.67					Cyclin-A1 putative expressed	LOC_Os01g13260.1	
135	GRMZM2G387360	4.12	5.52	2.69	4.02					LTPL160 - Protease inhibitor/seed storage/LTP family protein precursor	LOC_Os10g36170.1	
136	GRMZM2G398781			2.90	9.72					Uncharacterized protein	n/a	
137	GRMZM2G403915			8.64	2.92	5.37	2.50	6.55	2.01	*Nucleotide-sugar transporter family protein putative expressed	LOC_Os02g36390.4	
138	GRMZM2G422240	2.97	9.26							Heat shock protein 17.2	LOC_Os01g04370.1	
139	GRMZM2G470882	3.33	5.50							Uncharacterized protein	LOC_Os04g37760.1	
140	GRMZM2G476762					2.12	8.60	2.93	5.04	Uncharacterized protein	n/a	
141	GRMZM2G495234					2.81	2.48	2.19	3.44	Uncharacterized protein	n/a	
142	GRMZM5G851266	3.43	8.72							Putative polyphenol oxidase family protein	LOC_Os01g58100.1	
143	GRMZM5G862540	3.03	2.16							UDP-glucose 6-dehydrogenase	LOC_Os12g25700.1	
144	GRMZM5G892675	7.30	5.21							ATPase 3	LOC_Os12g24320.1	
145	GRMZM5G898668	4.69	2.94							*Exostosin family domain containing protein expressed	LOC_Os01g70200.1	
146	AC196158.3_FG002	-2.26	-2.92							Uncharacterized protein	n/a	
147	AC204539.4_FG003	-8.91	-3.39	-6.59	-4.65	-5.88	-3.79	-9.39	-3.31	*Profilin domain containing protein expressed	LOC_Os06g05880.1	
148	AC205886.3_FG001	-4.13	-2.51							*40S ribosomal protein S4 putative expressed	LOC_Os01g25610.1	
149	AC217050.4_FG007	-2.08	-6.76							TPS7 - terpene synthase 7	LOC_Os07g11790.1	
150	GRMZM2G005170	-2.36	-2.03	-2.19	-2.78					*MSP domain containing protein putative expressed	LOC_Os01g71050.1	
151	GRMZM2G005459	-3.70	-3.86			-2.96	-2.98			*RNA recognition motif containing protein putative expressed	LOC_Os01g71200.1	
152	GRMZM2G013920	-4.28	-6.84							Uncharacterized protein	n/a	
153	GRMZM2G021256	-5.10	-3.72	-4.60	-4.94	-3.49	-3.46	-3.29	-3.82	Oxygen evolving enhancer protein 3	LOC_Os02g36850.1	
154	GRMZM2G024738	-2.68	-2.01							Uroporphyrinogen decarboxylase	LOC_Os01g43390.1	
155	GRMZM2G028302	-6.18	-5.27	-4.98	-4.30	-3.24	-3.88	-3.80	-3.58	Uncharacterized protein	LOC_Os10g39150.1	
156	GRMZM2G028733	-3.88	-4.32	-3.23	-4.58	-3.71	-4.37	-3.20	-3.92	*Ubiquitin carboxyl-terminal hydrolase 6 putative expressed	LOC_Os01g36930.1	
157	GRMZM2G031204	-9.16	-9.58	-7.82	-5.31	-7.55	-7.36	-7.70	-8.79	Peptidyl-prolyl cis-trans isomerase	LOC_Os01g68710.1	
158	GRMZM2G036605	-3.59	#####	-3.79	#####	-4.70	#####	-4.79	#####	*Tetratricopeptide repeat domain containing protein expressed	LOC_Os02g01030.1	
159	GRMZM2G036880			-2.96	-3.13					Chlorophyll a-b binding protein 6A	LOC_Os06g21590.1	
160	GRMZM2G037334	-2.11	-8.58	-3.18	-4.75	-2.01	-6.02			*Remorin C-terminal domain containing protein putative expressed	LOC_Os02g44102.1	
161	GRMZM2G044851	-2.19	-2.45							*Peptide transporter PTR2 putative expressed	LOC_Os02g46460.1	
162	GRMZM2G045699	-4.29	#####							Uncharacterized protein	n/a	
163	GRMZM2G050875	-7.06	#####							Uncharacterized protein	n/a	
164	GRMZM2G056743	-2.39	-3.14							Uncharacterized protein	n/a	
165	GRMZM2G057491	-8.08	-9.59							*Glutamyl-tRNA synthetase cytoplasmic putative expressed	LOC_Os10g22380.1	
166	GRMZM2G060886			-2.70	-4.81					*CPuORF25 - conserved peptide uORF-containing transcript expressed	LOC_Os01g50030.1	
167	GRMZM2G061126	-9.07	-8.10	-7.92	#####	-7.66	-7.59	-5.51	-7.33	Uncharacterized protein	n/a	
168	GRMZM2G064374	-8.56	-6.22							Uncharacterized protein	n/a	
169	GRMZM2G067929	#####	-4.45	#####	-5.47			#####	-5.50	Uncharacterized protein	n/a	
170	GRMZM2G068707	-2.70	-5.44							Uncharacterized protein	n/a	
171	GRMZM2G072117	2.05	-2.53					-2.08	-2.62	AT-hook protein 1	LOC_Os10g42230.1	
172	GRMZM2G074083	-2.01	-2.43							*CBS domain containing membrane protein putative expressed	LOC_Os04g05010.1	
173	GRMZM2G074307	#####	-5.96	#####	-9.50	#####	-9.20	#####	-8.33	Uncharacterized protein	n/a	
174	GRMZM2G081192							-3.71	-2.68	Aquaporin PIP2-3	LOC_Os02g41860.2	
175	GRMZM2G082608			-2.32	-2.62					Uncharacterized protein	LOC_Os01g69840.1	
176	GRMZM2G091743	-2.85	-5.47	-5.31	-3.62					Uncharacterized protein	n/a	
177	GRMZM2G098460	-2.07	-3.24	-2.29	-2.38	-2.86	-2.72	-2.19	-3.30	Drought-induced protein 1	LOC_Os02g30320.1	
178	GRMZM2G100568	-4.53	-4.02							*Expressed protein	LOC_Os02g14500.1	
179	GRMZM2G106429							-2.11	-2.13	*DnaK family protein putative expressed	LOC_Os11g47760.1	
180	GRMZM2G106795			-2.34	-2.45	-2.74	-2.46	-2.19	-3.34	ADP-ribosylation factor	LOC_Os02g47110.1	
181	GRMZM2G107082							-2.27	-2.05	*ATP-grasp domain containing protein expressed	LOC_Os11g47330.1	
182	GRMZM2G108527	-3.88	-5.27							Uncharacterized protein	n/a	
183	GRMZM2G110553	-2.67	-4.40							Uncharacterized protein	n/a	
184	GRMZM2G115491							-2.46	-2.74	Cupin domain containing protein expressed	LOC_Os02g32980.1	
185	GRMZM2G115698	-6.28	-7.70							*Expressed protein	LOC_Os02g14500.1	
186	GRMZM2G116966	-2.00	-3.84			-2.15	-4.38			Benzoate carboxyl methyltransferase	LOC_Os06g13350.1	
187	GRMZM2G131315	-3.41	-4.96			-5.38	-5.34	-7.57	-6.68	*OsSCP4 - Putative Serine Carboxypeptidase homologue expressed	LOC_Os01g43890.1	
188	GRMZM2G132577	-5.86	-3.99	-5.32	-5.11	-4.14	-3.93	-3.92	-3.51	Uncharacterized protein	LOC_Os01g38660.1	
189	GRMZM2G133203	-2.03	-2.05							Uncharacterized protein	LOC_Os02g40040.1	
190	GRMZM2G134340	-7.66	-7.73	-6.34	-8.71	-7.61	-7.53	-8.71	-6.36	Uncharacterized protein	n/a	
191	GRMZM2G135132					-3.47	-2.85	-3.88	-5.19	*Kinase pfkB family putative expressed	LOC_Os02g41590.1	
192	GRMZM2G137493			-8.63	-2.50					Uncharacterized protein	n/a	
193	GRMZM2G137696	#####	#####	#####	-8.46	-8.64	#####	#####	#####	*DnaK family protein putative expressed	LOC_Os02g48110.1	
194	GRMZM2G138248	-3.08	-6.81							CYP9 - Cytochrome P450 family 9	LOC_Os03g37290.1	
195	GRMZM2G157822	-6.70	-6.19	#####	#####	-7.65	-7.34	-5.96	-7.37	*Myosin putative expressed	LOC_Os03g64290.1	
196	GRMZM2G165308	-4.90	-5.04	-3.20	-6.36	-3.26	-5.29			Uncharacterized protein	n/a	
197	GRMZM2G318992	-6.56	-4.49	-4.34	-2.62	-6.08	-4.69	-5.46	-2.73	*KIP1 putative expressed	LOC_Os05g39000.1	
198	GRMZM2G338696	-5.64	-8.01							Cytochrome c oxidase subunit 5B mitochondrial precursor putative expressed	LOC_Os01g42650.1	
199	GRMZM2G343636	-5.19	-3.61			-3.39	-3.51	-2.94	-2.56	*NAD dependent epimerase/dehydratase family protein putative expressed	LOC_Os03g23980.1	
200	GRMZM2G351248	-2.70	-4.79							*NAD dependent epimerase/dehydratase family protein putative expressed	LOC_Os03g23980.1	
201	GRMZM2G356839	-2.79	-7.03							Uncharacterized protein	n/a	
202	GRMZM2G371079	-3.84	-3.12	-2.98	-3.35					Uncharacterized protein	LOC_Os01g69870.1	
203	GRMZM2G374302					-3.16	-3.42			Pyridoxal-dependent decarboxylase protein putative expressed	LOC_Os04g01690.1	
204	GRMZM2G400961			-2.24	-2.18					Uncharacterized protein	LOC_Os04g55610.1	
205	GRMZM2G411216	-5.24	#####							Uncharacterized protein	n/a	
206	GRMZM2G429972	-5.26	#####	-5.79	#####	-5.84	#####	-5.65	#####	Uncharacterized protein	n/a	
207	GRMZM2G457347	-9.63	#####	#####	-9.39	-6.75	#####	-8.05	-8.22	Uncharacterized protein	LOC_Os03g58590.1	
208	GRMZM2G587231	-2.32	-7.48							Uncharacterized protein	n/a	
209	GRMZM2G702522	-7.45	-6.77	-8.46	-5.74	-7.33	-5.42	-9.19	-7.68	Uncharacterized protein	n/a	
210	GRMZM5G815851	-3.49	-2.34							Uncharacterized protein	n/a	
211	GRMZM5G876518					#####	-5.16			40S ribosomal protein S4 putative expressed	LOC_Os01g25610.1	
212	GRMZM5G877929	-3.94	#####							Uncharacterized protein	n/a	
213	GRMZM5G883813	-5.90	-2.02							Uncharacterized protein	n/a	
214	GRMZM5G890040	-4.31	-6.61							Uncharacterized protein	n/a	
215	GRMZM5G897005	-3.87	-9.76	-3.86	#####	-3.37	#####	-3.70	#####	*Protein kinase domain containing protein expressed	LOC_Os01g02790.1	